

Addressing Phenomenological Diffusion Problems with the Lattice Monte Carlo Method

Graeme E. Murch, Irina V. Belova and Thomas Fiedler

University Center for Mass and Thermal Transport in Engineering Materials
The University of Newcastle
New South Wales
Australia

Research supported by the Australian Research Council

Outline

- 1. Introduction to the Lattice Monte Carlo (LMC) method.**
- 2. Some examples of applications of the LMC method to the calculation of effective mass diffusivities and concentration profiles.**
- 3. Some examples of applications of the LMC method to the calculation of effective thermal conductivities and temperature profiles.**
- 4. Concluding remarks.**

The Lattice Monte Carlo (LMC) method

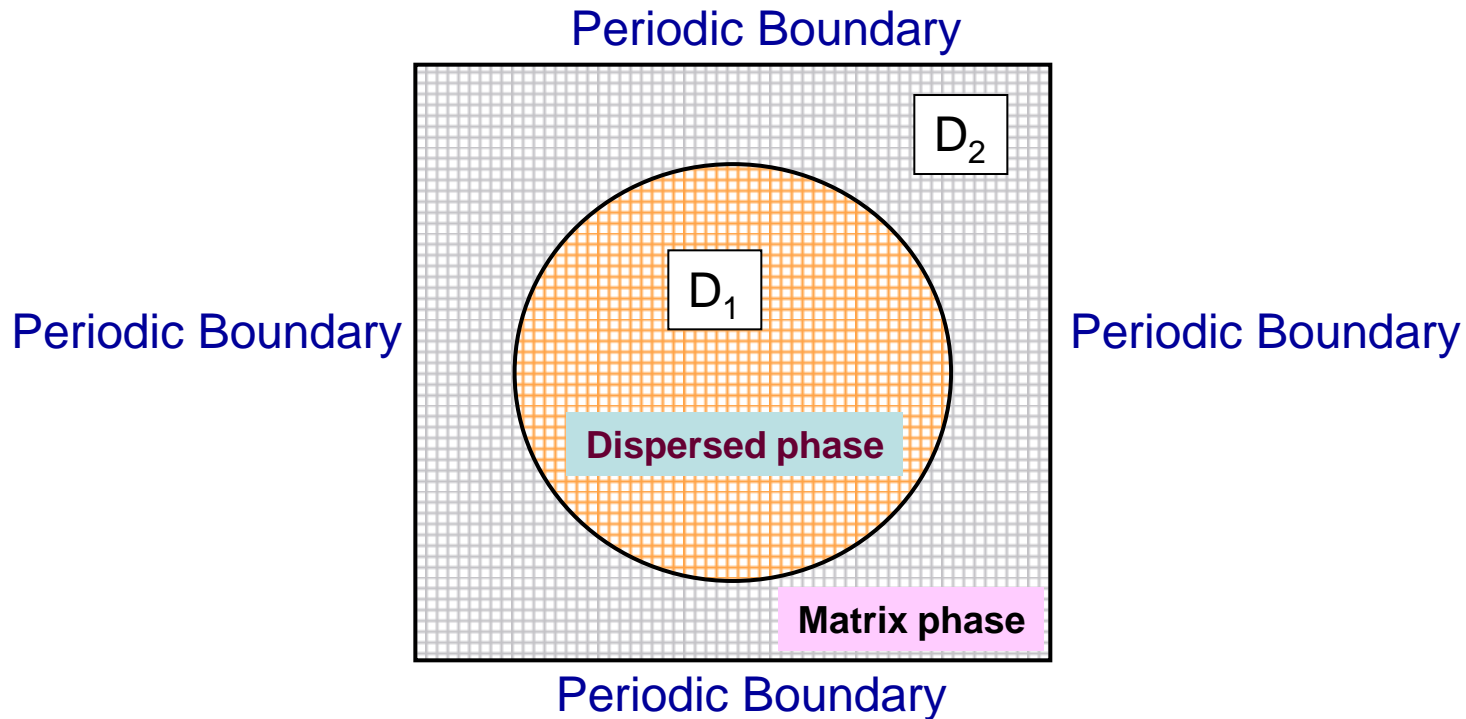
- **Basic concept**: A phenomenological mass (or thermal) diffusion problem is mapped onto a very fine-grained lattice which is then explored by random walking mass or energy ‘packets’. Multiple occupancy of sites by packets is required.

Individual mass and thermal diffusivities in the problem are very easily described by using the uncorrelated random walk expression:

$$D \rightarrow \Gamma s^2 / 6$$

- The site to site distance s in this lattice can be rescaled to any real distance ranging from nano scales to micro or even macro-scales.
- The method is called the ‘**Lattice Monte Carlo**’ method to distinguish it from the atomistic ‘**Kinetic Monte Carlo**’ method.

How to calculate an effective diffusivity.



Question:

A composite has a spherical dispersed phase that has a different diffusivity from the matrix. What is the effective diffusivity of the composite?

Solution:

Map the problem onto a very fine grained lattice which is then explored by a large number, say 10^5 , mass packets all taking random walks. The 'jump rate' of the packets is made proportional to the diffusivities D_1 and D_2 in each phase.

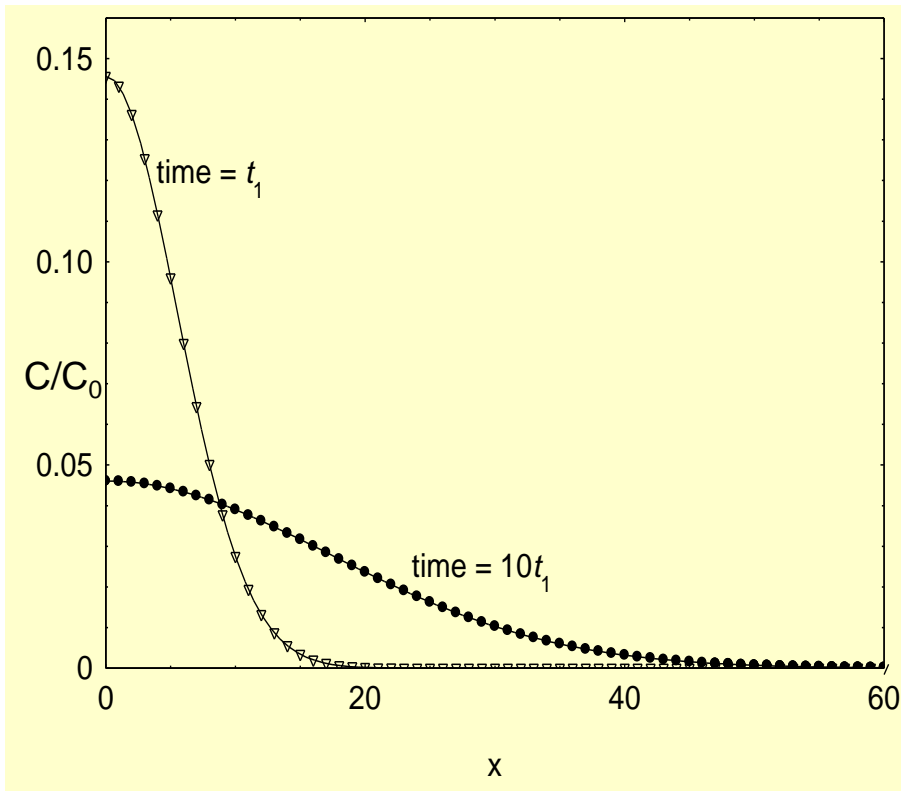
The effective diffusivity of the composite is obtained in the long-time limit with the Einstein Equation:

$$D = \langle R^2 \rangle / 6t$$

$\langle R^2 \rangle$ is the mean square displacement of the mass packets in time t

How to calculate a concentration profile

Concentration profiles can be easily assembled by counting the number of mass packets that have reached a given location after starting from a source, or sources, after some time t .



Typical Gaussian concentration profiles for tracer diffusion from an 'instantaneous' or thin-film source' at $x=0$
Points: LMC,
Lines: exact solution.

Recent applications of the LMC method for addressing phenomenological diffusion problems.

- **Effective thermal conductivities and diffusivities in cellular metals using computer tomography scans of real materials mapped onto the LMC lattice. Phase-change materials.**
- **Concentration profiles and effective mass and thermal diffusivities in model composites.**
- **Coupled mass and thermal diffusion (Soret effect) temperature and concentration profiles.**
- **Concentration profiles for models of diffusion with reaction.**
- **Concentration profiles and effective diffusivities for grain boundary and interphase boundary diffusion models.**
- **Interdiffusion concentration profiles in binary alloys.**
- **Ionic conductivity in composite electrolytes.**

Review articles: I V Belova, G E Murch, T Fiedler, A Öchsner, *Diffusion Fundamentals*, 4, pp15.1 - 15.23 (2007), on-line and *Prog. Chemical Eng, Studium Press*, 2010.

**Some examples of applications of the LMC method
to mass diffusion**

The diffusion coefficient is a function of position

Example of diffusion in grains and grain boundaries

Tracer Concentration Depth Profiles in the Presence of Grain Boundaries:

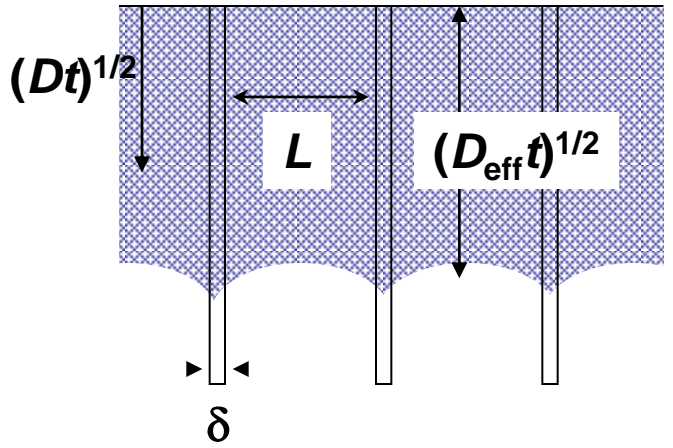
- **Short-circuit diffusion via grain boundaries is traditionally described by parallel grain boundary 'slabs' arranged normal to the surface.**
- **Three basic kinetics regimes were recognized by Harrison:**

Type-A, B and C kinetics regimes.

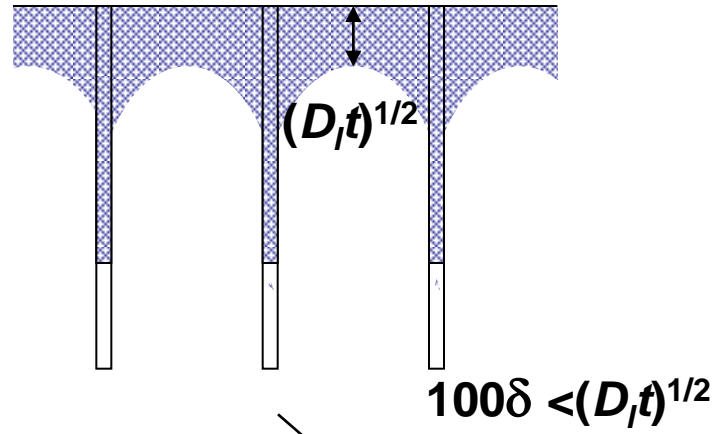
(Additional transgrain boundary diffusion regimes AB and BC have also been identified since.)

The Harrison Type - A, B and C kinetics regimes for tracer diffusion from a thin-film source at the surface into a medium containing grain boundaries:

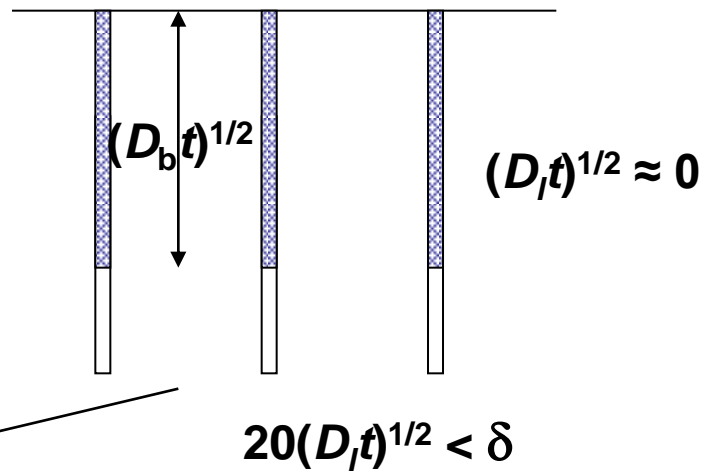
Type-A



Type-B



Type-C

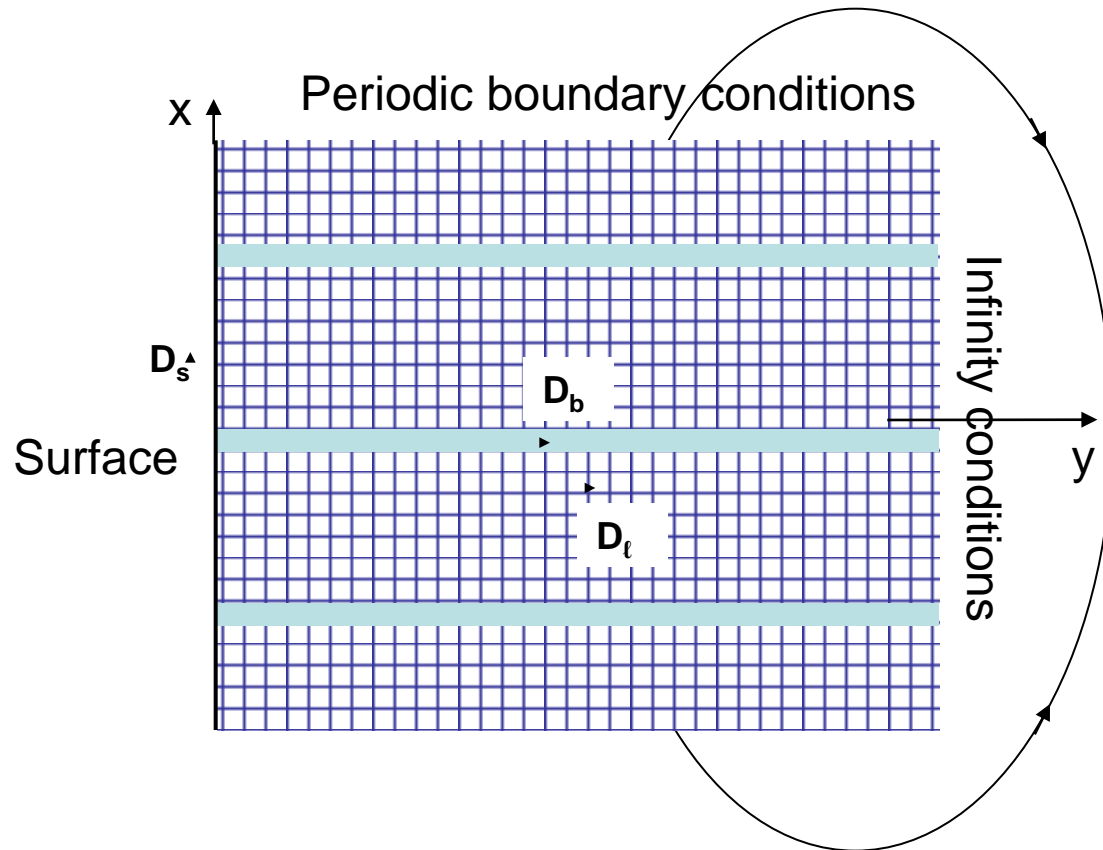


$(D_l t)^{1/2} \gg L$
Get D_{eff}

Get D_l
 (from first region)
 and
 δD_b
 (from tail region)

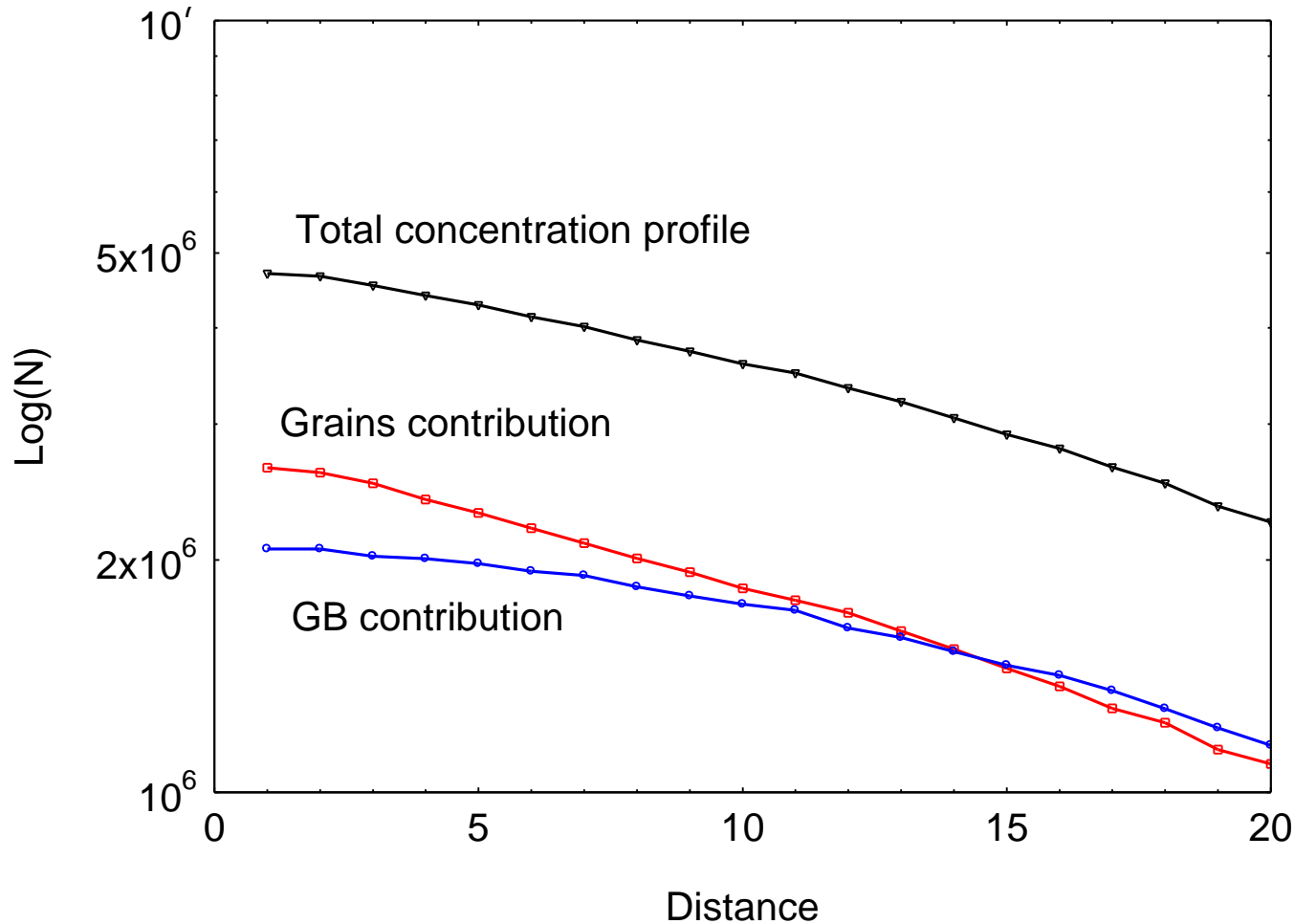
Get D_b

Grain boundary diffusion in the parallel slabs model



Actual mesh size used in LMC is very much finer than that shown.

Typical LMC (log) concentration profile for the Type-A kinetics regime
Black solid line with triangles – total concentration
Red line with squares – lattice or bulk (grains) contribution
Blue line with circles – grain boundary contribution

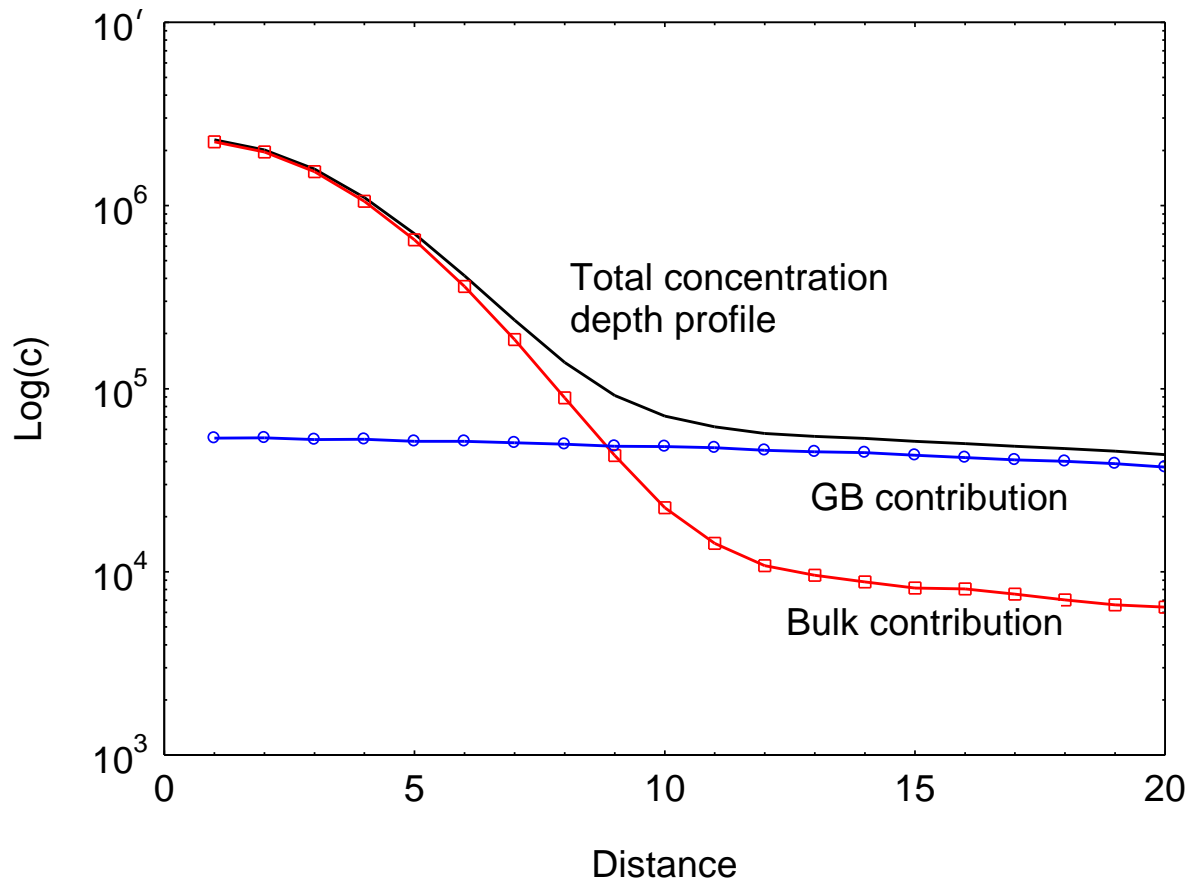


Typical LMC (log) concentration profile for the Type-B kinetics regime ($\Lambda = 20$)

-Black solid line – total concentration

-Red line with squares – lattice or bulk (grains) contribution

-Blue line with circles – grain boundary contribution



The transition from Harrison Type-A kinetics to Type-B kinetics (end of Type-A kinetics): Parallel slabs model

This transition was originally estimated by Harrison to occur for spherical grains at:

$$\Lambda = L/(D_1 t)^{1/2} = 0.0033.$$

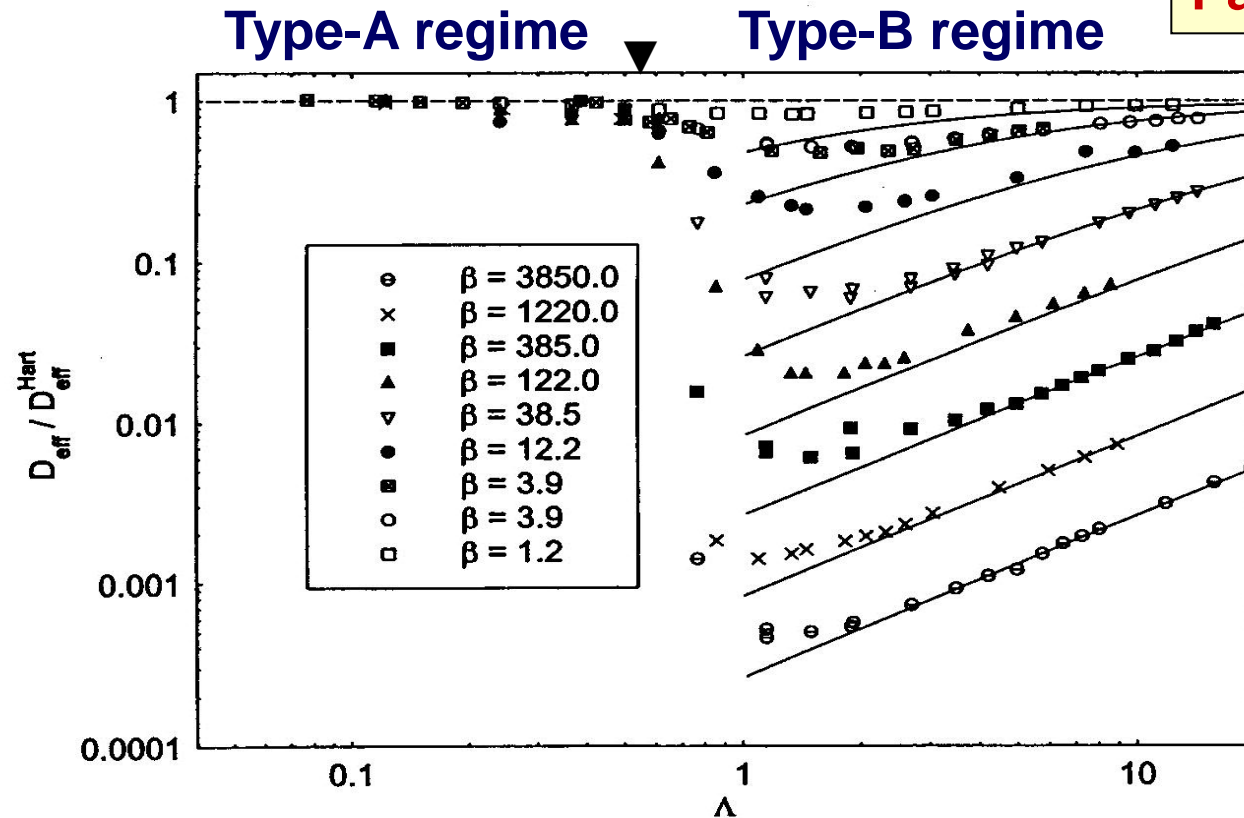
This estimate was later refined to $\Lambda = 0.1$ (Gupta *et al.* 1978). That analysis was later found to contain mathematical inconsistencies (Kaur *et al.* 1995)).

LMC determination of the transition from Harrison Type-A kinetics to Type-B kinetics (end of Type-A kinetics): Parallel slabs model

The essence of the LMC calculation is to analyze the concentration profiles themselves in order to determine D_{eff} .

This D_{eff} is then compared with the D_{eff} given by the Hart Equation (which is exact for parallel grain boundary slabs) in the Type-A regime:

$$D_{\text{eff}}^{\text{Hart}} = g D_b + (1-g) D_l$$

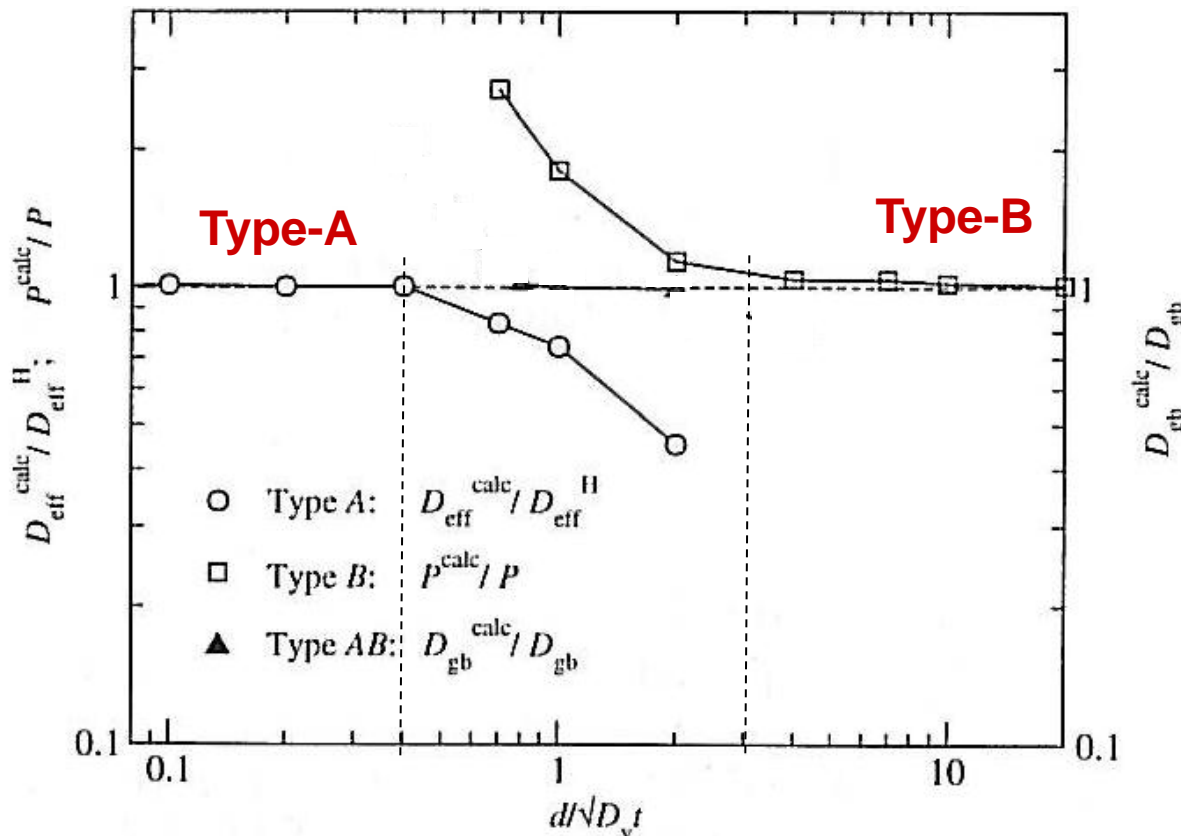


$D_{\text{eff}}/D_{\text{eff}}^{\text{Hart}}$ as a function of Λ ($= L/(D_i t)^{1/2}$) for various values of β (slow surface diffusion model). Solid lines correspond to the Harrison Type-B kinetics condition ($D_{\text{eff}} = D$).

The transition from Type-A occurs at $\Lambda \approx 0.4$ and depends slightly on the β or ‘Le Claire’ parameter $= \delta D_b/2D_i\sqrt{D_i t}$.

LMC was later used to study the the Type-A, intermediate Type-AB and Type-B kinetics regimes (Divinski *et al.*, *Zeit. Metallk.*) $P (= \delta D_b)$ was used to delineate the Type-B kinetics regime.

Λ was changed by manipulating the grain size. $\Delta = D_b / D = 10^5$; $\beta = 500$



Conclusions:

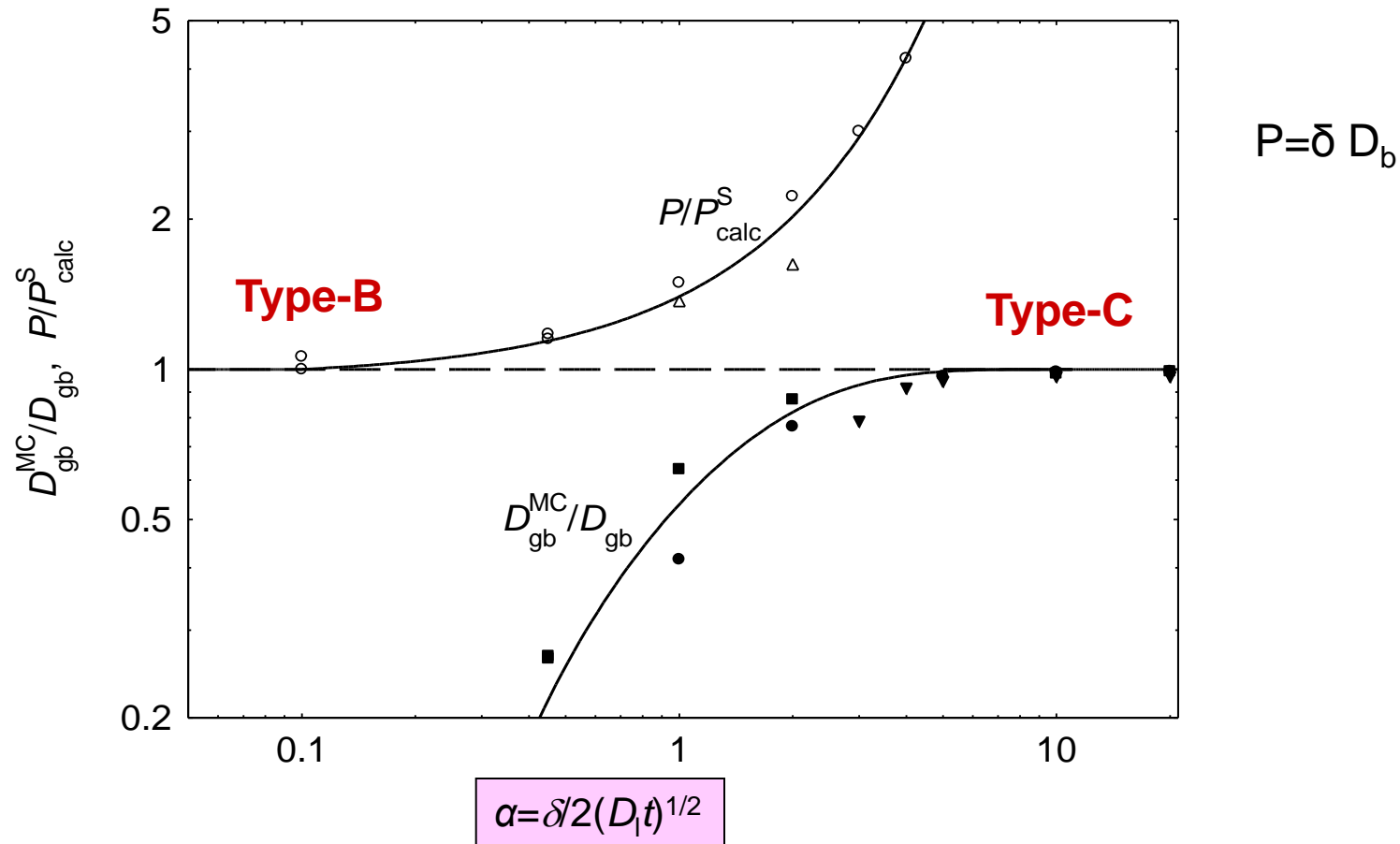
Type-A: $\Lambda \leq 0.4$

Type-AB: $0.4 \leq \Lambda \leq 3.0$

Type-B: $3.0 \leq \Lambda$

Type-B to Type-C kinetics

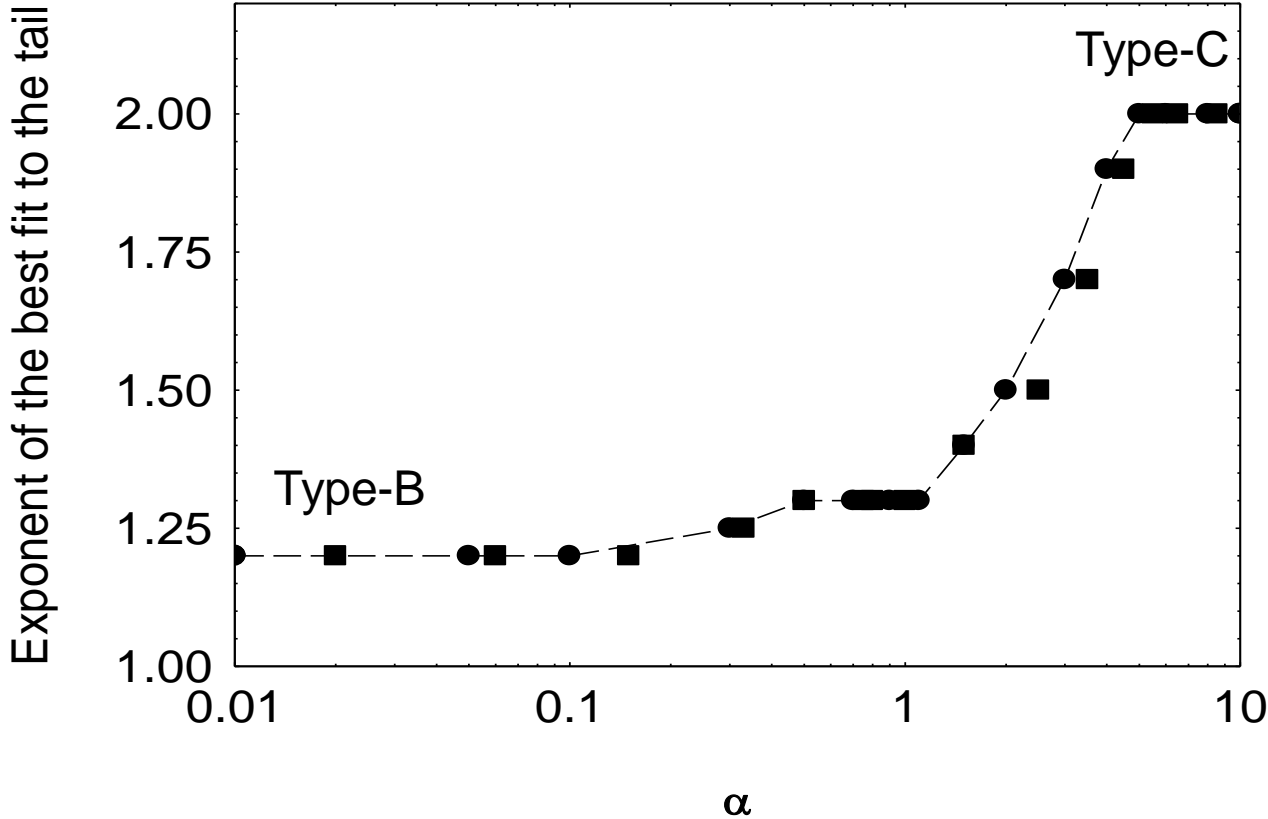
Parallel slabs model



P/P^S_{calc} and D_{gb}^{MC} / D_{gb} as functions of α for various values of Δ and β for the case of the parallel slabs model for the grains. $\Delta = 10 - 4000$.

Δ : $\bullet - \Delta = 10^5$; $\blacksquare - \Delta = 10^4$; $\blacktriangledown - \Delta = 10^6$; $\circ - \Delta = 10^4$; $\triangle - \Delta = 10^5$. **Belova and Murch, Phil Mag 2009.**

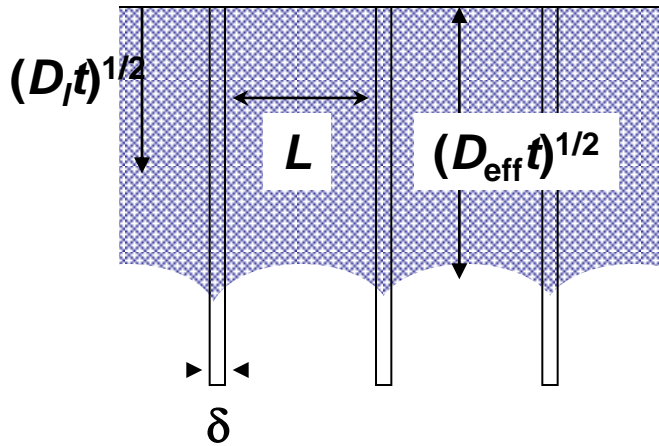
Type-B to Type-C kinetics



The overall best-fit exponent to the profile simply changes 'fairly smoothly' from 1.2 to 2.0 when α increases from 0.1 to 5.0.

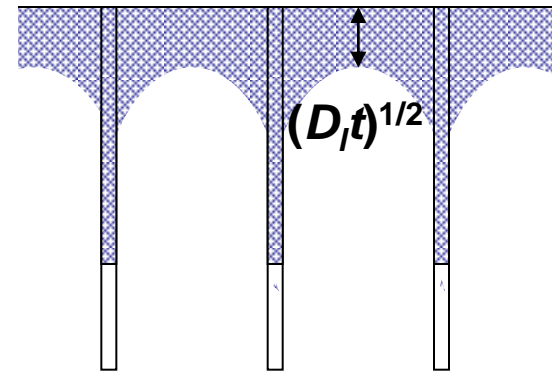
Refinements to the limits of the Harrison Type - A, B and C kinetics regimes, **parallel slabs model**, self-diffusion:

Type-A



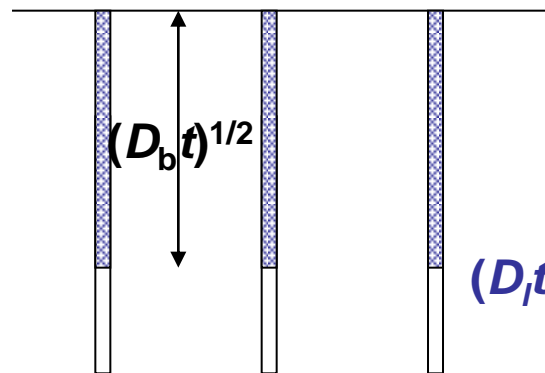
$(D_t t)^{1/2} \gg L$

Type-B



$100\delta < (D_t t)^{1/2}$

Type-C



$(D_t t)^{1/2} \approx 0$

$20(D_t t)^{1/2} < \delta$

Refined to:
 $5\delta \leq (D_t t)^{1/2} \leq 0.33L$

Refined to: $10(D_t t)^{1/2} \leq \delta$

Refined to:
 $(D_t t)^{1/2} \geq 2.5L$

Parallel slabs model

Harrison Type-A kinetics regime.

Thus, it is clear that $\sqrt{(D_1t)}$, needs to be only greater than two and half times the spacing between the (parallel) grain boundary slabs for the concentration profile to be in the Harrison Type-A kinetics regime and for the effective diffusivity to be described by the Hart Equation.

Harrison Type-B kinetics regime.

It is also clear that to be sure the diffusion experiment is in the Type-B kinetics regime, $\sqrt{(D_1t)}$ needs to be less than one third of the spacing between the grain boundary slabs.

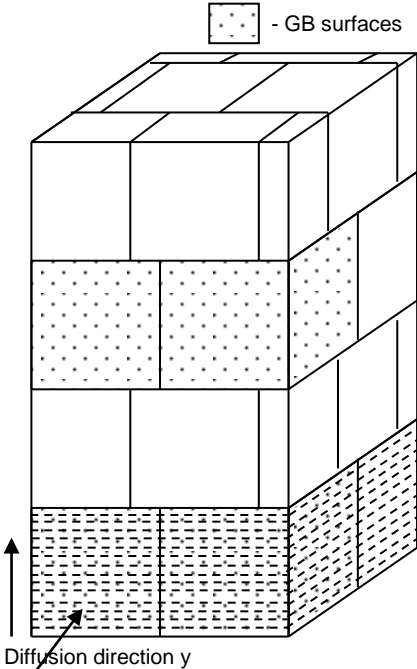
But there is a conceptual problem with the parallel grain boundary slabs model:

In the Harrison Type-A kinetics region in the diffusion anneal time a typical tracer atom can be expected to encounter a number of grain boundaries normal to the diffusion direction.

According, LMC investigations have been extended to closed grain models.

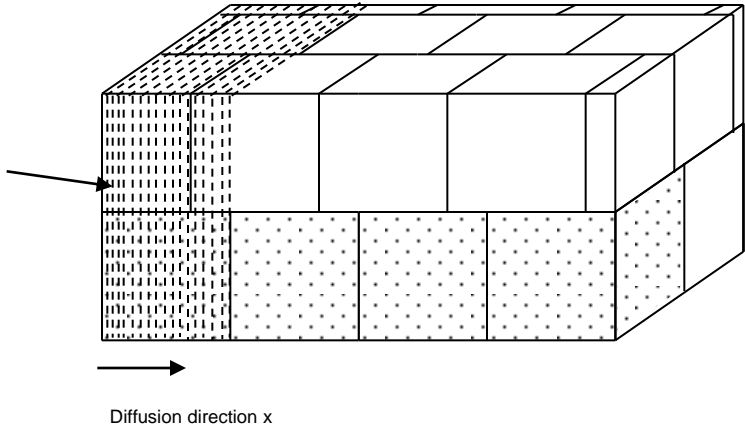
Closed (Cubic) Grain model

- Grain models:**
- a) diffusion is in the y direction, (the source plane is at $y = 0$).
 - b) diffusion is in the x direction (the source plane is at $x = 0$).



(a)

Instantaneous source plane positions



(b)

First of all, what is the effective diffusivity for a closed grain model?

Closed (Cubic) Grain model

In general, LMC testing on various closed grain models has shown that the **Hart Equation (1951)** is actually a pretty poor approximation for D_{eff} .

Fortunately, extensive LMC testing showed that the **Maxwell-Garnett Equation (1895)** describes D_{eff} very well:

$$D_{eff} = \frac{D_b (2g(D_b - D_l) + 3D_l)}{gD_l + (3 - g)D_b}$$

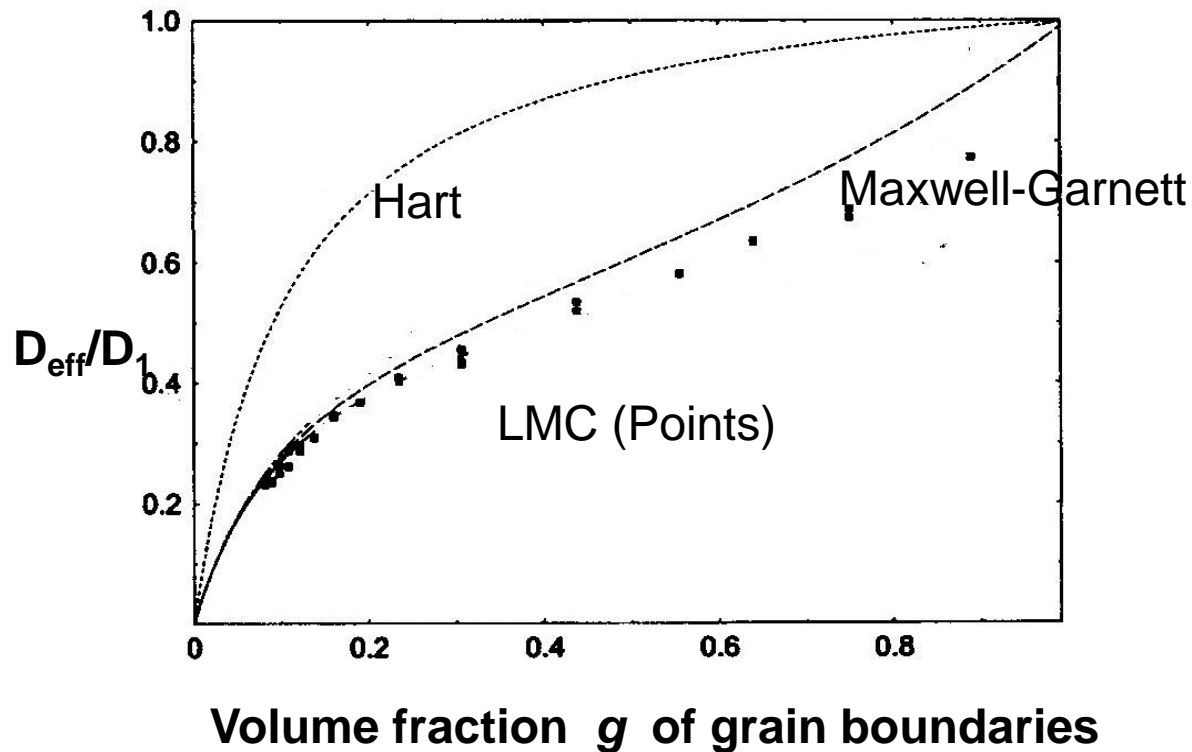
LMC calculation of the effective diffusivity in the presence of closed cubic grains.

Generalized Hart Equation:

$$\frac{D_{eff}}{D_l} = (1 - g)D_l + gD_b$$

Maxwell-Garnett Equation:

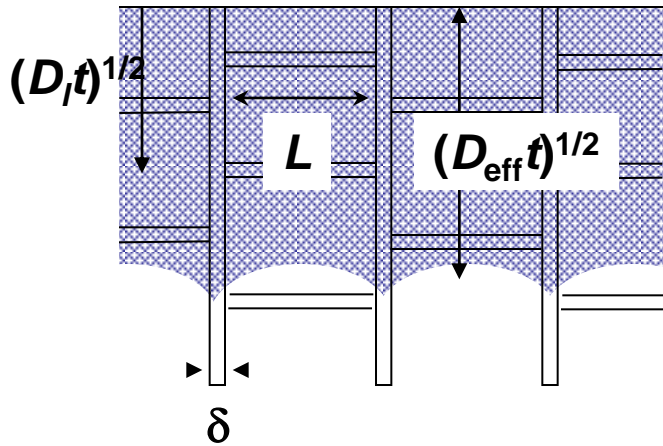
$$\frac{D_{eff}}{D_l} = \frac{2(1 - g)D_l + (1 + 2g)D_b}{(2 + g)D_l + (1 - g)D_b}$$



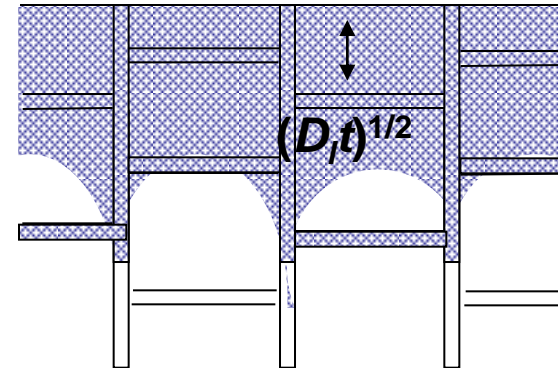
$D_b/D_l = 10^3.$

The Harrison Type - A, B and C kinetics regimes, Cubic grains model, self-diffusion:

Type A



Type B

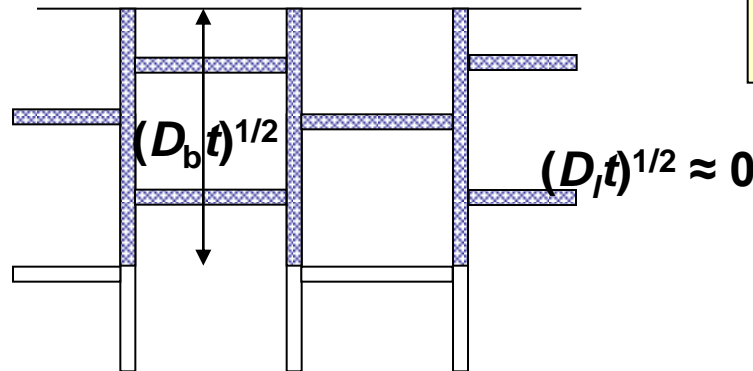


The diffusion length $(D_i t)^{1/2}$ needs to be less than 0.16 times the grain size to be sure of being in Regime B.

$(D_i t)^{1/2} \gg L$

Refined to:
 $(D_i t)^{1/2} \geq 0.3L$

Type C

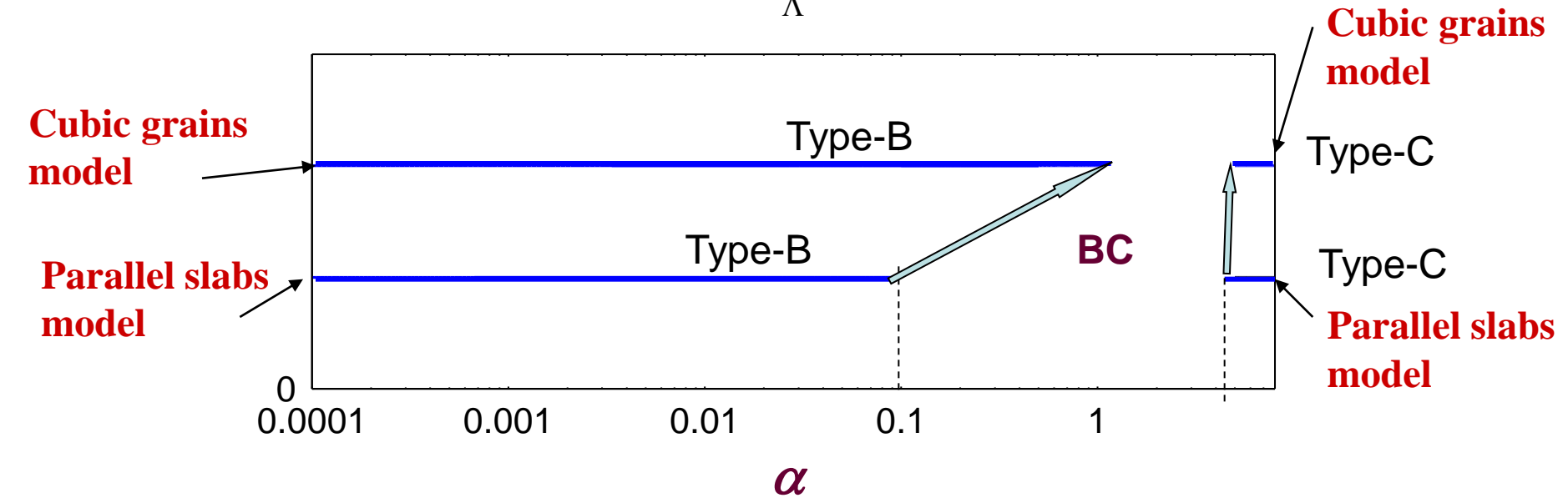
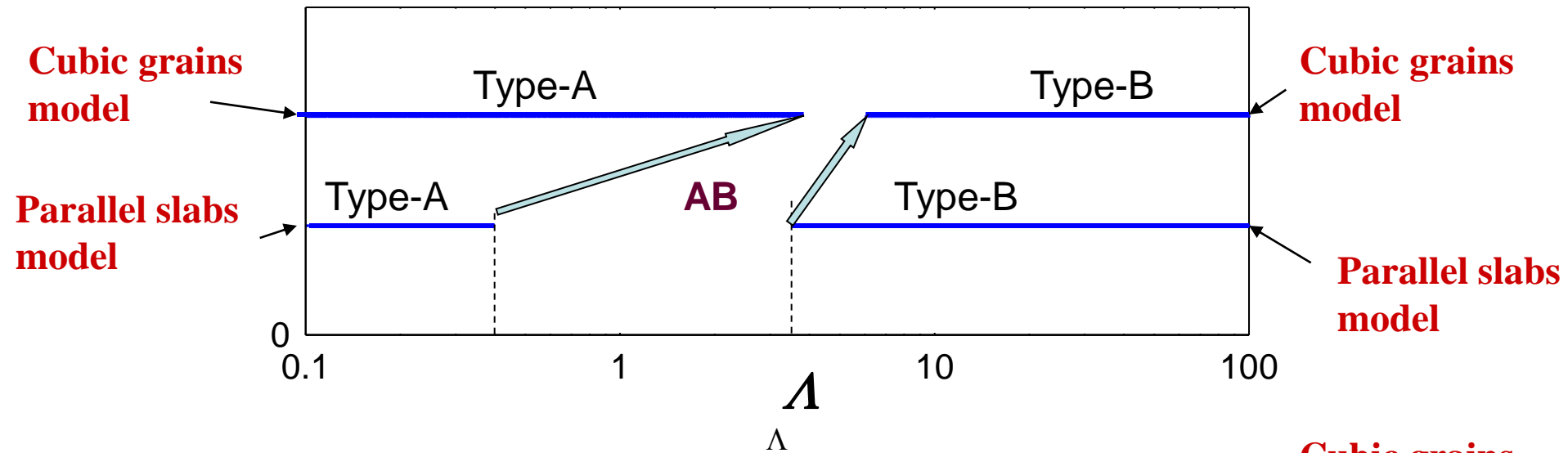


$100\delta < (D_i t)^{1/2}$

Refined to:
 $\delta \leq (D_i t)^{1/2} \leq 0.16L$

$20(D_i t)^{1/2} < \delta \rightarrow$ Refined to: $10(D_i t)^{1/2} \leq \delta$

Limits of the Harrison kinetics regimes: Self-diffusion



Cubic grains model

Harrison Type-A kinetics regime.

$\sqrt{(D_1 t)}$, needs to be only greater than one third the spacing between the grains for the concentration profile to be in the Harrison Type-A kinetics regime.

Harrison Type-B kinetics regime.

To be certain that the diffusion experiment is actually in the Type-B kinetics regime, $\sqrt{(D_1 t)}$ needs to be less than one sixth of the spacing between the grains.

This finding is disturbing because it means that many experiments on polycrystalline material may possibly have not been performed in the Type-B regime and therefore have a significant grain boundary contribution to the measured diffusivity.

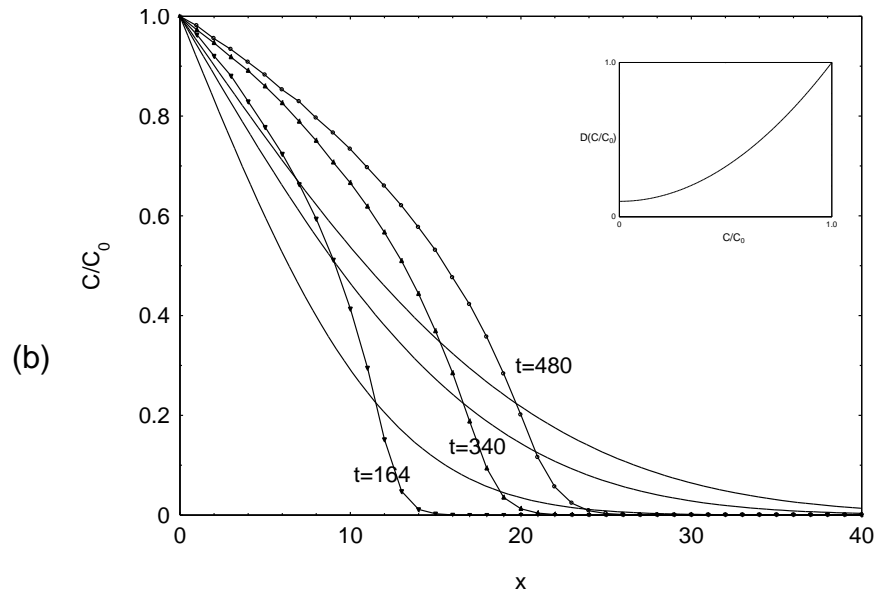
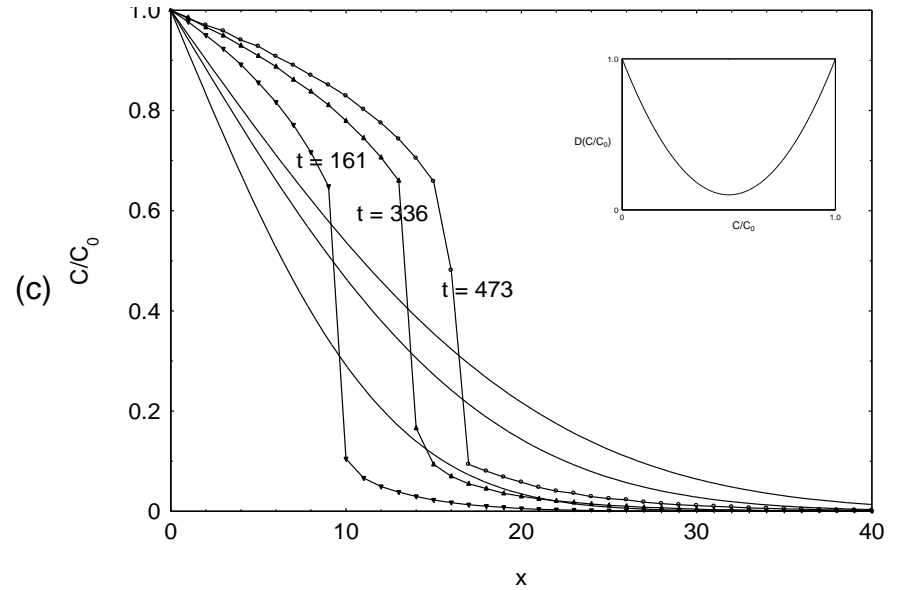
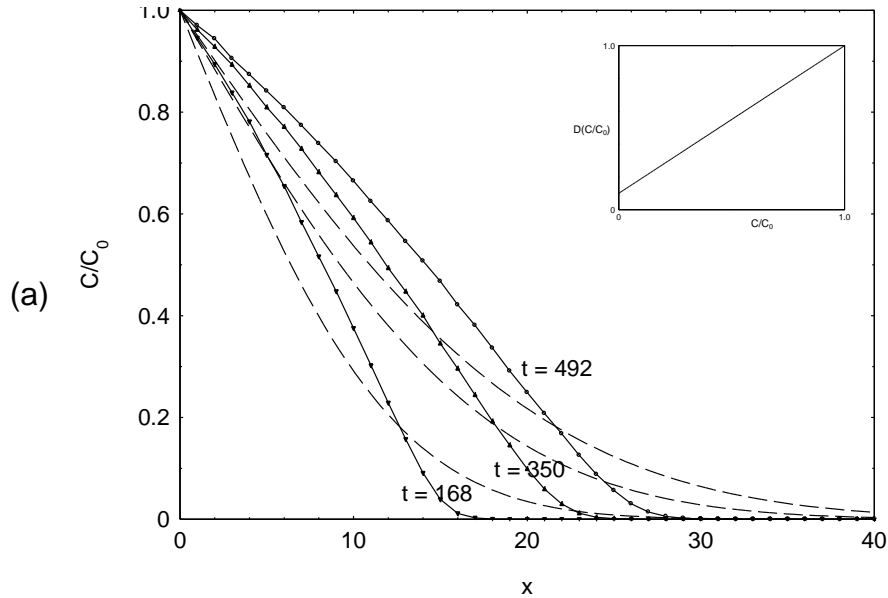
**Diffusion coefficient depends on concentration
(non-linear diffusion).**

Incorporating a concentration dependence of the various diffusivities into LMC

In a great many diffusion problems, the diffusivities are functions of concentration.

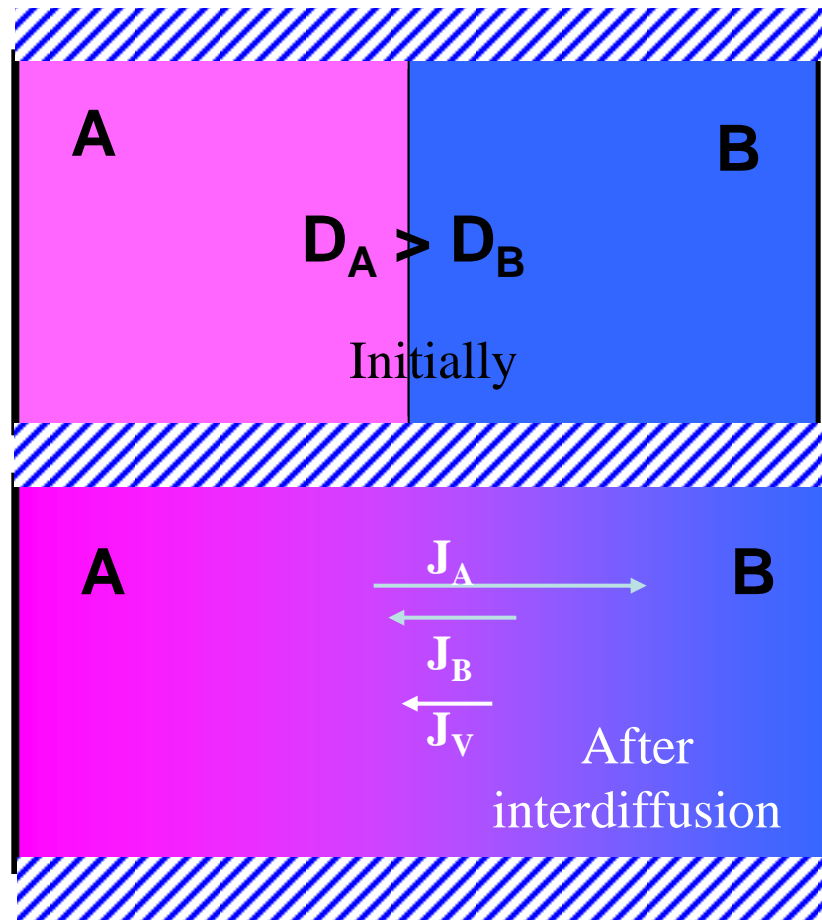
This is very easily incorporated into LMC by relating the local jump rate Γ_i (and therefore the local D_i) at a site i to the actual local concentration at site i (i.e. the total number of mass packets presently at that site relative to the number at some reference, e.g. the source).

LMC calculation of some concentration profiles: $D=D(C)$



Concentration profiles for diffusion of a diffusant from a constant source when $D=D(C)$:
a) linear;
b) and c) quadratic concentration dependence.

Interdiffusion concentration profiles in a binary diffusion couple from the interdiffusion coefficient.



A Kirkendall shift occurs because of the inequality of the atomic fluxes.

LMC laboratory frame calculation that gives a Kirkendall shift of the interdiffusion concentration profile:

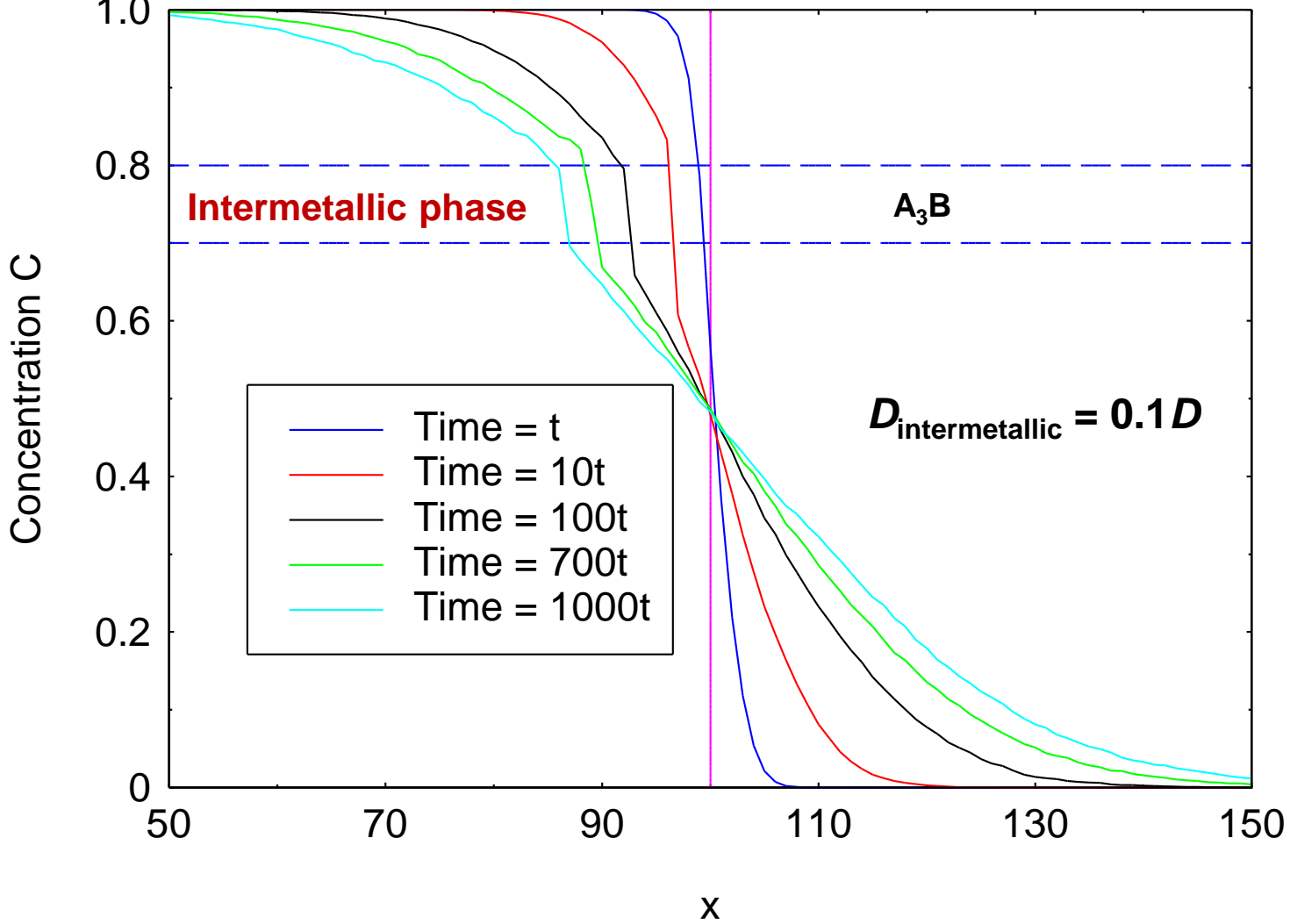
- In this reference frame, we have two types of species (A and B). Mass packets of A and B are moved independently but in such a way that the total composition ($c_A + c_B$) is always kept constant at a site.
- The concentration dependence of the interdiffusion coefficient is manipulated by proxy by changing the jump rate of each species packet independently:

$$\tilde{D}(c_A) = c_B D_A(c_A) + c_A D_B(c_A)$$

This method automatically gives the correct Kirkendall shift when $D_A \neq D_B$.

LMC determination of interdiffusion concentration profiles with the formation of an intermetallic A_3B (grows parabolically),

Belova et al. DDF 2011



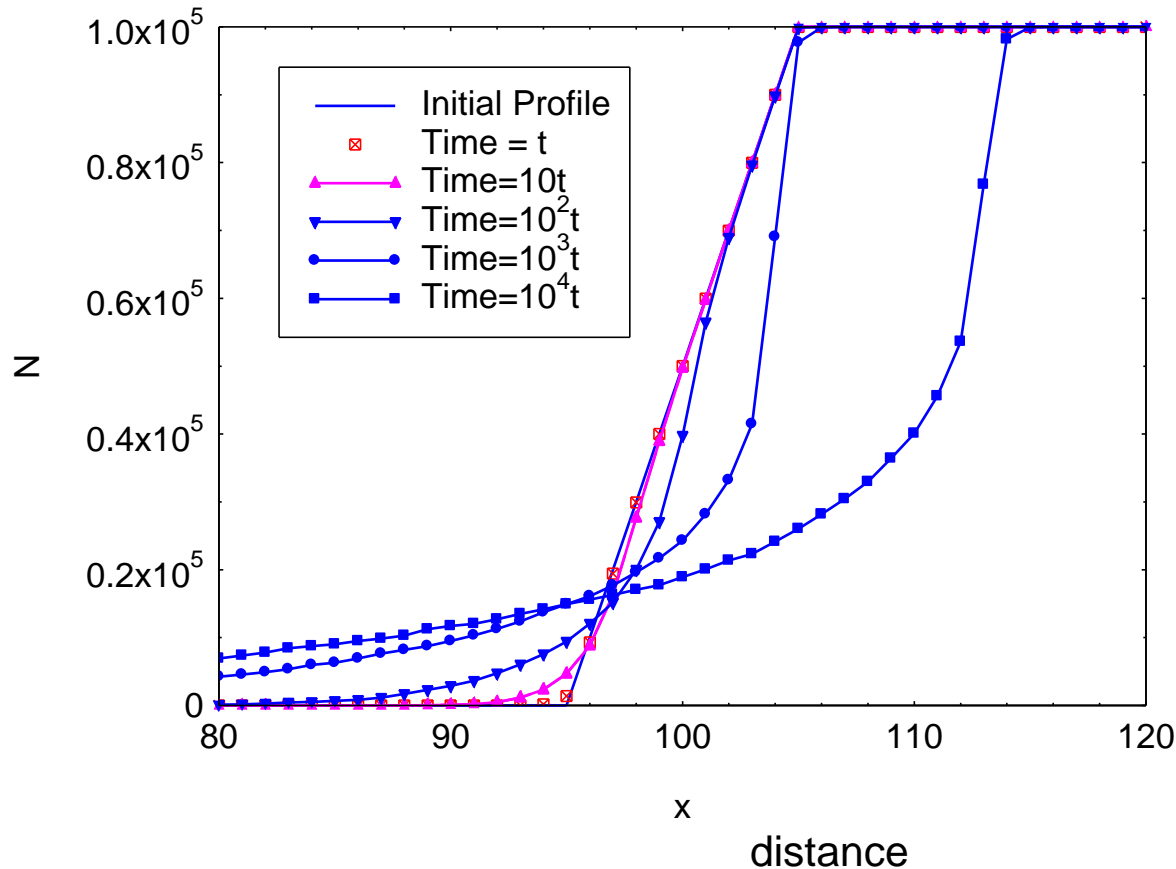
Interface sharpening

In some completely miscible alloys, an anomalous sharpening (apparent 'uphill diffusion') of an initially diffuse interface has been observed in e.g.

- **The Cu-Ni system (growth of Ni on Cu)** (Erdelyi et al. Surf. Sci. (2002),
- **The Mo-V system** (Erdelyi et al. Science, 2004).

Atomistic Kinetic Monte Carlo simulations suggested that interface sharpening is caused by a very strong exponential dependence of the interdiffusivity and that it is a special 'nano' effect. Erdelyi et al. Surf. Sci. (2002).

LMC illustration of the interface sharpening effect.
The initial interface is diffuse (assumed first to be linear)
and $D(C) = D(0) \exp(-8C)$ Belova et al. DDF 2010.



This is not really uphill diffusion (even though it looks a little like it!)
The linear profile at t=0 is highly inconsistent with this particular $D(C)$
and the profile is then ‘repaired’ during the diffusion anneal.

The phenomenon of **interface sharpening** is, in principle, a perfectly general diffusion phenomenon.

It need not be confined to the nano-scale though there may be morphological reasons why it may not occur at higher scales.

Numerical analysis of an experimental concentration profile to obtain D(C), Belova and Murch, 2011 to be publ.

1. Boltzmann-Matano analysis (1935):

$$-\frac{\lambda}{2} \frac{dC}{d\lambda} = \frac{d}{d\lambda} \left(D(C) \frac{dC}{d\lambda} \right)$$

$$D(C) = -\frac{1}{2} \frac{\int_{c_1}^c \lambda dC}{(dC/d\lambda)_c}$$

2. Proposed alternative analysis:

J.S. Kirkaldy: Mat. Sci. Eng A, 222, 104 (2006):

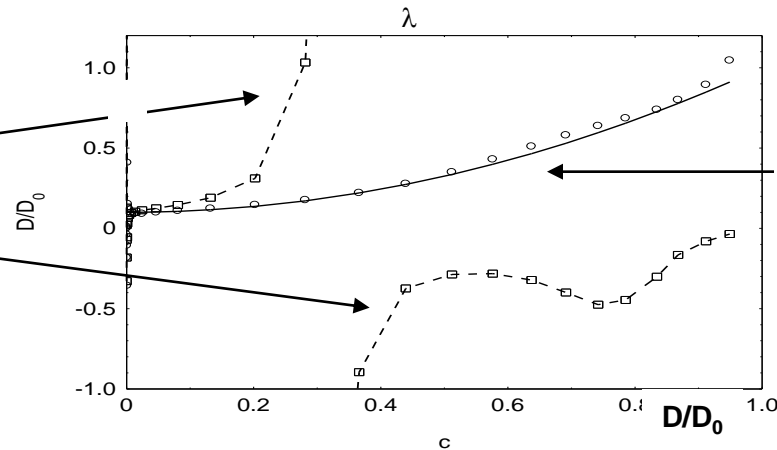
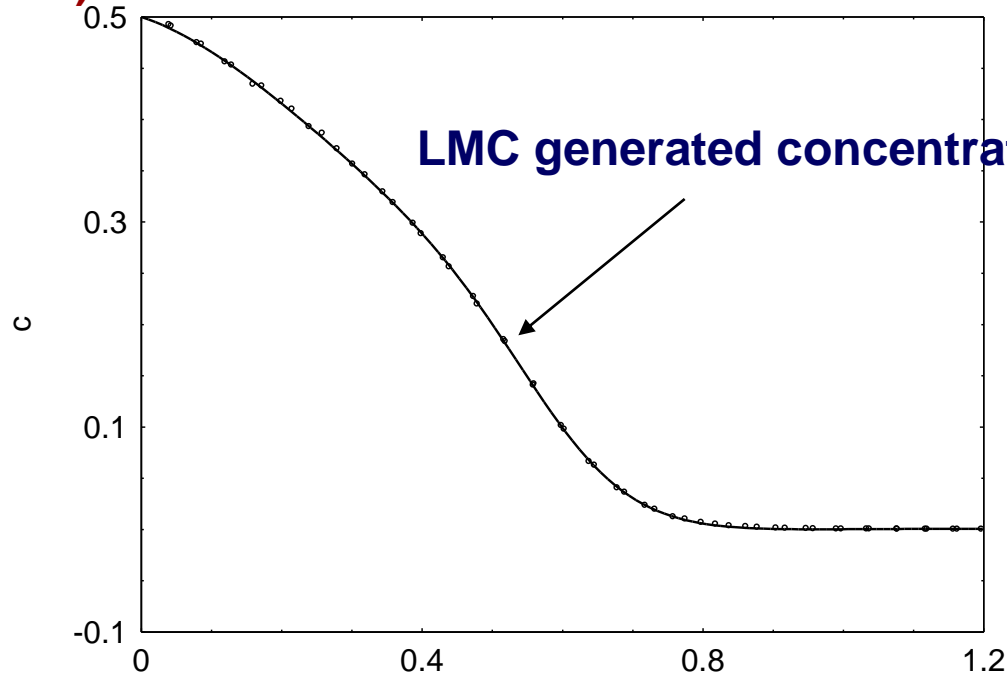
$$-\frac{\lambda}{2} \frac{dC}{d\lambda} = D(C) \frac{d}{d\lambda} \left(\frac{dC}{d\lambda} \right)$$

We can test these two analyses to obtain D(C) side-by-side in the following way:

- Put D(C) into a LMC calculation.
- Generate the concentration profile.
- Process the generated profile with both analyses to test the recovery of the original D(C).

Quadratic dependence of the diffusion coefficient

$$D = D_0(1 + a c^2)$$

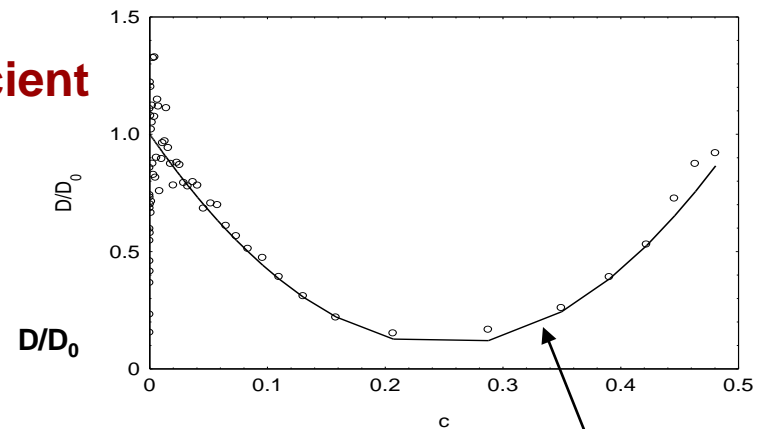
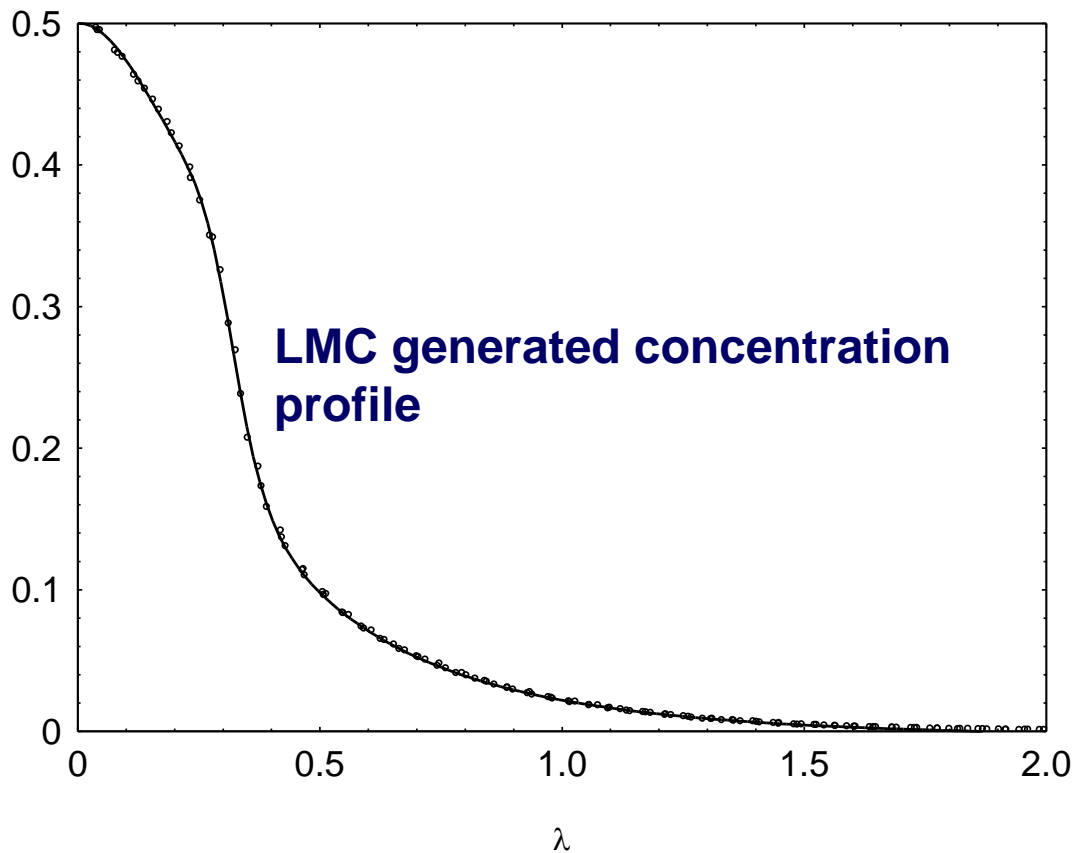


**Solid line: Input $D(C)$.
Points: Boltzmann-Matano
analysis using the LMC
profile**

**Alternative analysis
using LMC profile**

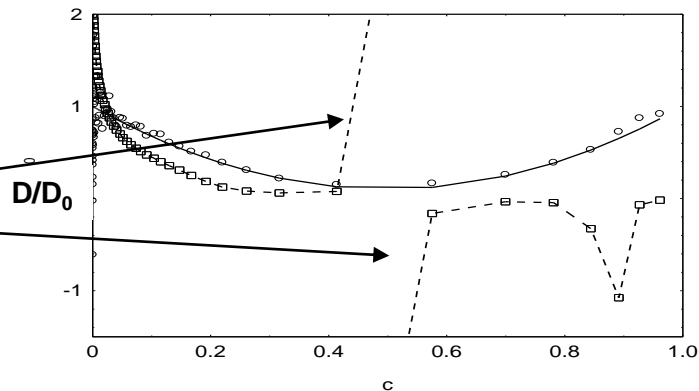
Quadratic dependence of the diffusion coefficient

$$D = D_0(1 + a c (1 - c))$$



Solid line: Input $D(c)$.
Points: Boltzmann-Matano analysis using the LMC profile

Alternative analysis using LMC profile



Result: The Boltzmann-Matano analysis is superior and robust.

Mass diffusion with chemical reaction

Different types of chemical reaction

- Instantaneous reaction:

- Constant ratio R of reactants and products

$$\frac{\partial a}{\partial t} = D \frac{\partial^2 a}{\partial x^2} - \frac{\partial c}{\partial t} = D \frac{\partial^2 a}{\partial x^2} - R \frac{\partial a}{\partial t}$$

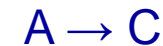


A fraction of mobile A reacts instantly with immobile B to form immobile C.

- Irreversible reaction:

- Reaction rate k_1

$$\frac{\partial a}{\partial t} = D \frac{\partial^2 a}{\partial x^2} - k_1 \cdot a$$



A reacts irreversibly with B to form C with rate k_1 .

- Reversible reaction:

- Reaction rate k_1 , reverse reaction rate k_2

$$\frac{\partial a}{\partial t} = D \frac{\partial^2 a}{\partial x^2} - k_1 \cdot a + k_2 \cdot c$$



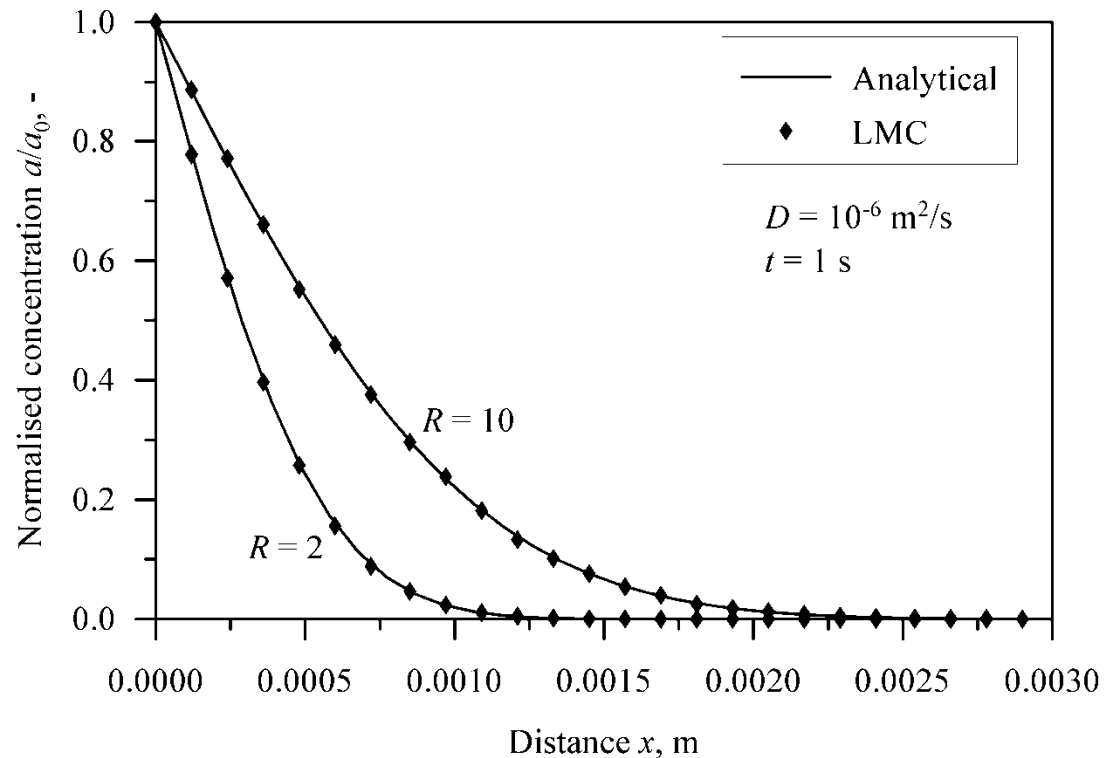
A reacts reversibly with B to form C.

Instantaneous reaction

- Corrected diffusivity

$$D' = \frac{D}{R + 1}$$

Constant species ratio R updated at each time step.

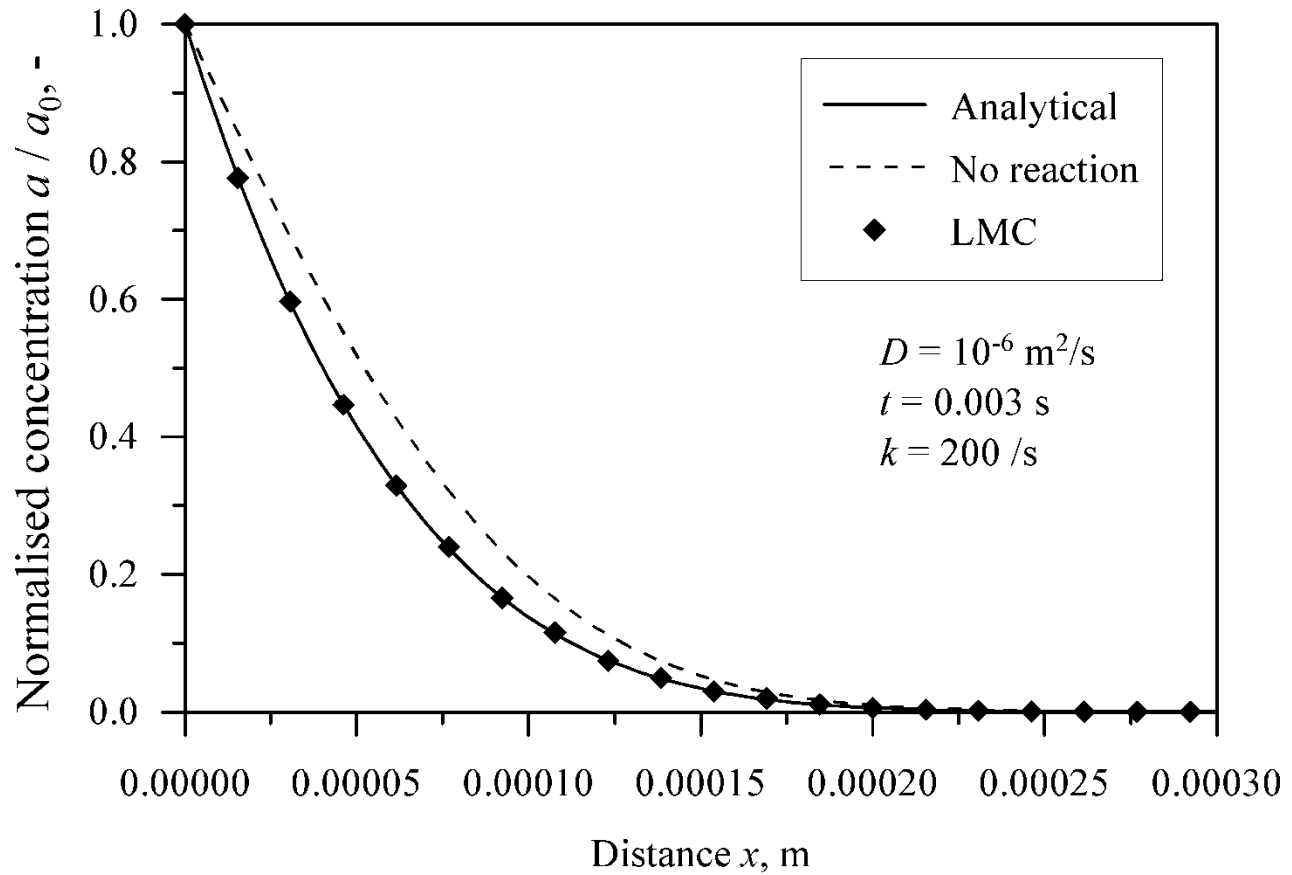


Irreversible reaction

- Diffusion into a semi-infinite medium with a constant surface concentration
- Exact solution:

$$a(x, t) = \frac{a_0}{2} \cdot \left\{ \exp\left(-x \cdot \sqrt{\frac{k}{D}}\right) \cdot \operatorname{erfc}\left(\frac{x}{2\sqrt{Dt}}\right) - \sqrt{kt} \right. \\ \left. + \exp\left(-x \cdot \sqrt{\frac{k}{D}}\right) \cdot \operatorname{erfc}\left(\frac{-x}{2\sqrt{Dt}}\right) + \sqrt{kt} \right\}.$$

Irreversible reaction



Reversible reaction

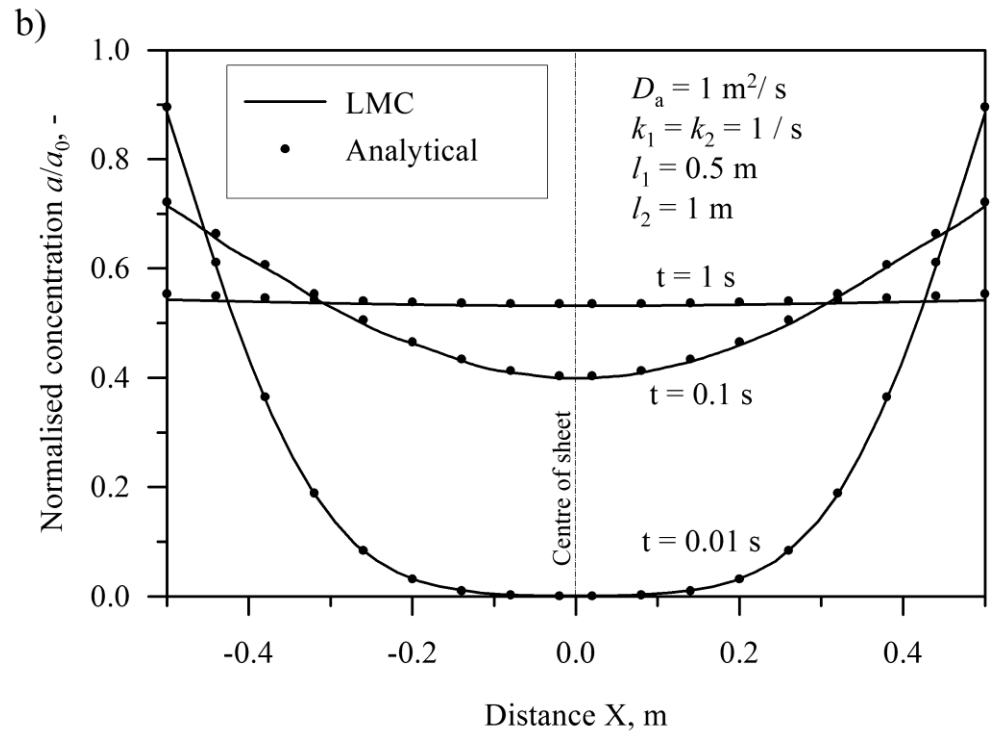
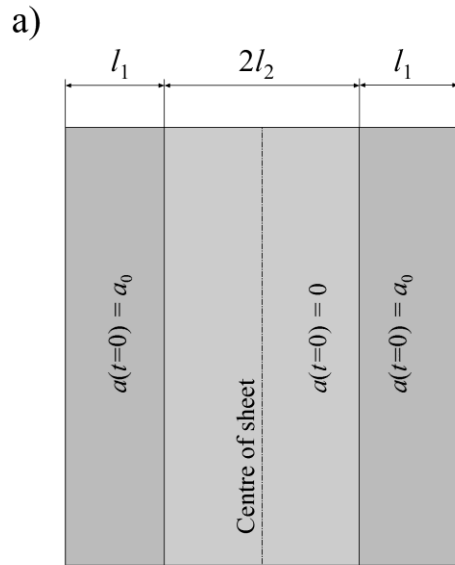
- Infinite sheet of known thickness suspended between two layers of solute that contain the reactants.
- Analytical solution

$$a(x, t) = \frac{l_1 \cdot a_0}{l_1 + \left(\frac{k_2}{k_1} + 1\right) \cdot l_2} + \sum_{n=1}^{\infty} \left[\frac{a_0 \exp(\alpha_n t)}{1 + \left(1 + \frac{k_1 k_2}{(\alpha_n + k_1)^2}\right) \left(\frac{l_2}{2l_1} + \frac{\alpha_n}{2D\beta_n^2} + \frac{\alpha_n^2 l_1 l_2}{2D^2 \beta_n^2}\right)} \cdot \frac{\cos \beta_n x}{\cos \beta_n l_2} \right]$$

$$\frac{l_1 \alpha_n}{D_A} = \beta_n \tan \beta_n l_2,$$

$$\beta_n^2 = -\frac{\alpha_n}{D_A} \cdot \frac{\alpha_n + k_1 + k_2}{\alpha_n + k_1}.$$

Reversible reaction



Some applications of the LMC method to thermal diffusion.

LMC Calculations of the Effective Thermal Diffusivity/Conductivity

Thermal diffusion, like mass diffusion, is a random process that can be represented by random walks. In the case of thermal diffusion, the packets are now virtual thermal energy packets.

The Einstein Equation also describes the thermal diffusivity K in d dimensions ($d = 1,2,3$):

$$K = \frac{\langle R^2 \rangle}{2dt}$$

Note: in a thermal diffusion context, the Einstein Equation has no physical meaning.

It purely provides a useful means for calculating the effective thermal diffusivity (conductivity) from random walks of virtual thermal energy packets.

It should be noted that:

The thermal conductivity λ_i in a phase i is directly related to the thermal diffusivity K_i in that phase by:

$$K_i = \lambda_i / \rho_i C_{p,i}$$

where ρ_i is the density of phase i and $C_{p,i}$ is its specific heat.

In a model composite, by simply requiring that the densities and the specific heats take values equal to unity everywhere in the calculation, the effective thermal conductivity λ_{eff} then simply trivially equals the effective thermal diffusivity K_{eff} .

The LMC Method for Determining Temperature Profiles

The amount of thermal energy E_p corresponding to a *virtual thermal energy packet* is given by:

$$E_p = T_c \cdot s^3 \cdot \rho \cdot C_p \cdot \frac{1}{N_p}$$

where s is the distance between two neighbouring lattice sites and N_p is the number of virtual thermal packets in the source plane.

Random walks are directed by two parameters:

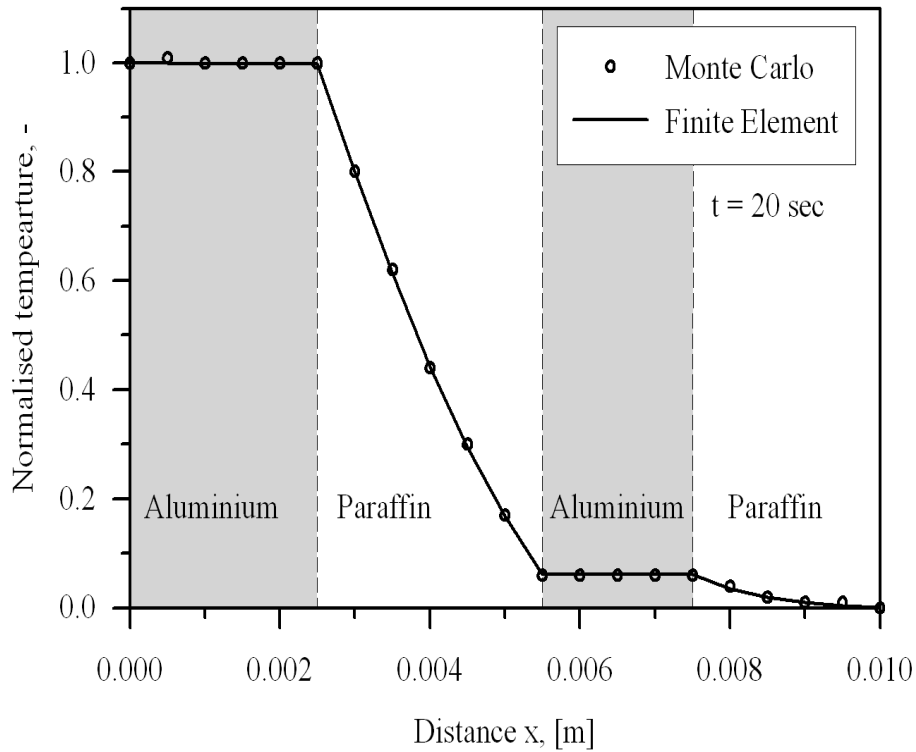
1. The jump probability p_j (scaled thermal conductivity) must be scaled with respect to the highest thermal conductivity:

$$p_{j,i} = \lambda_i / \lambda_{\max}$$

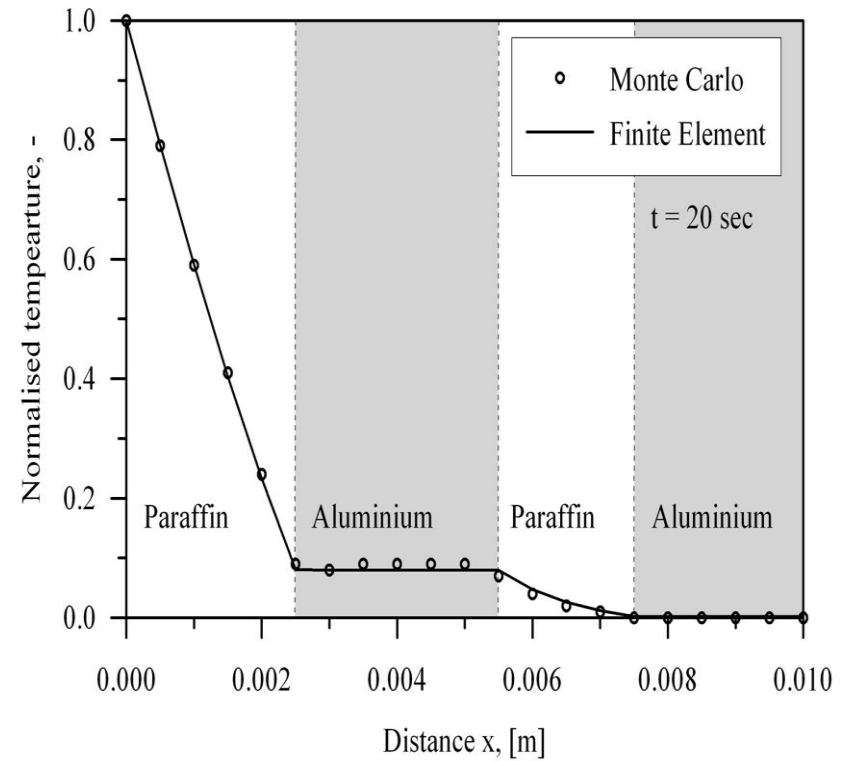
2. the selection probability p_s (scaled inverse product $\rho_i \cdot C_{p,i}$).

The selection probability is treated as an 'amount of inertia' assigned to a virtual thermal packet in a particular phase: i.e. the higher the specific heat in the phase the slower the virtual thermal energy packet.

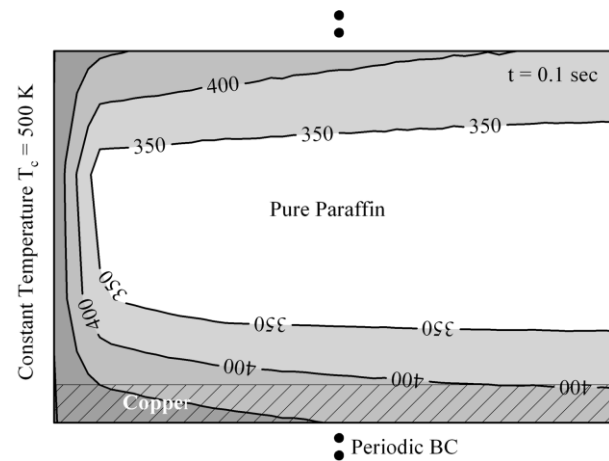
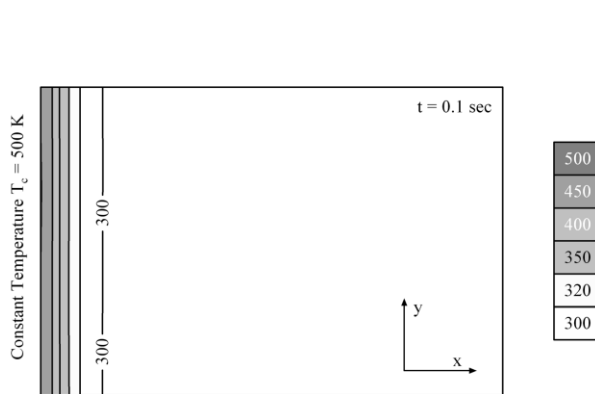
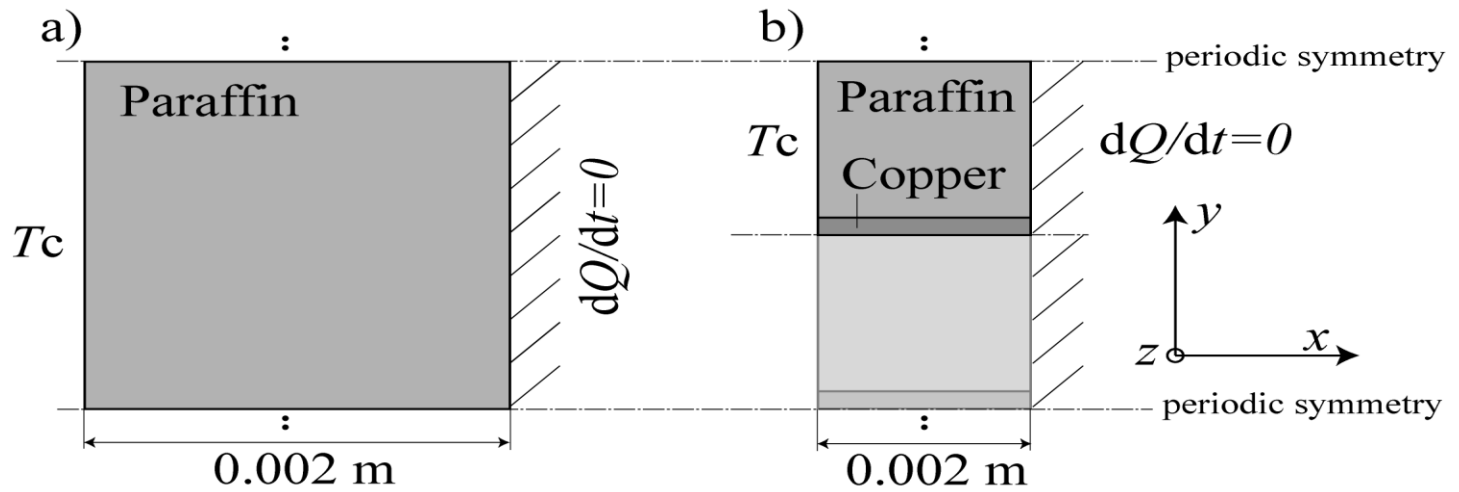
Comparison of LMC and FEA determinations of temperature profiles in layered aluminium / paraffin composites.



Temperature profile in a layered two-phase aluminium – paraffin composite (constant surface temperature).



Temperature profile in a layered two-phase paraffin - aluminium composite (constant surface temperature).



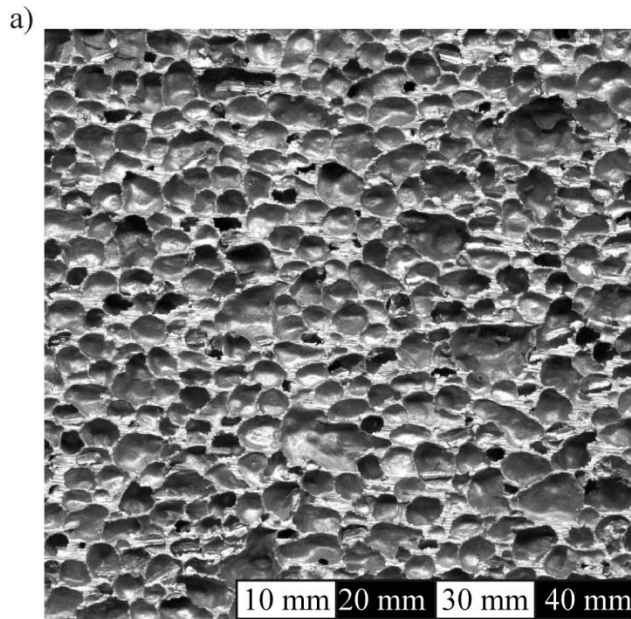
LMC two-dimensional temperature maps (constant temperature source at the surface):

a) pure paraffin,

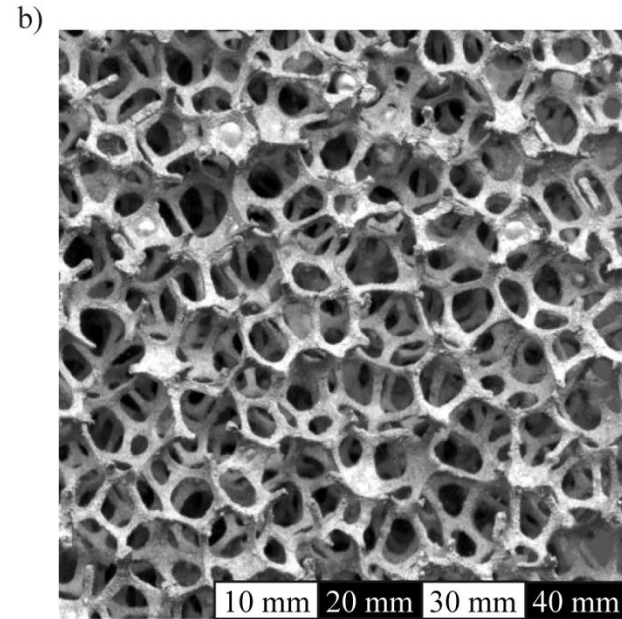
b) copper-paraffin composite.

Thermal diffusion in cellular metals

LMC determination of the effective thermal conductivity of a cellular metal.

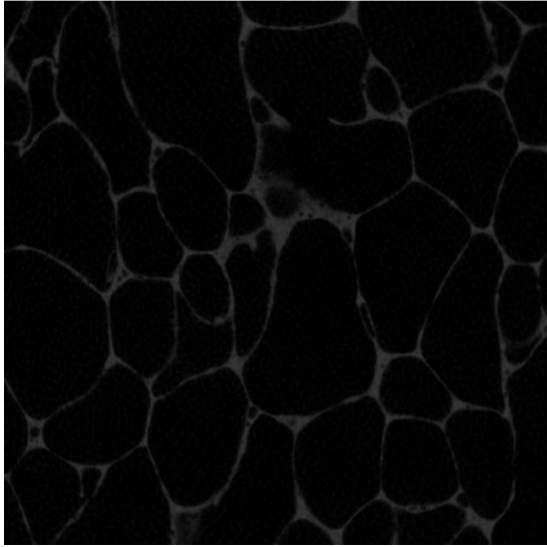


M-pore

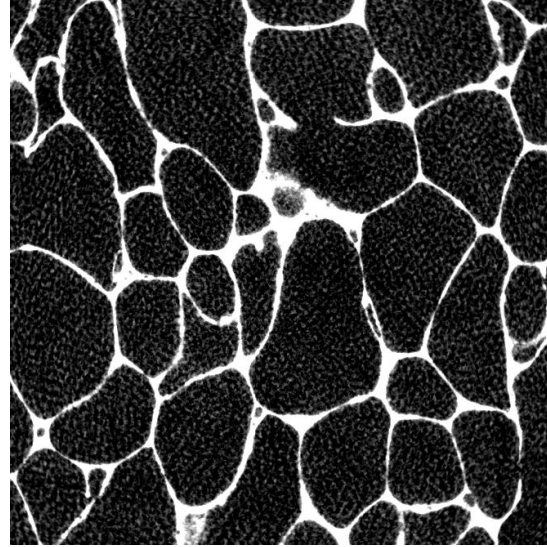


Alporas

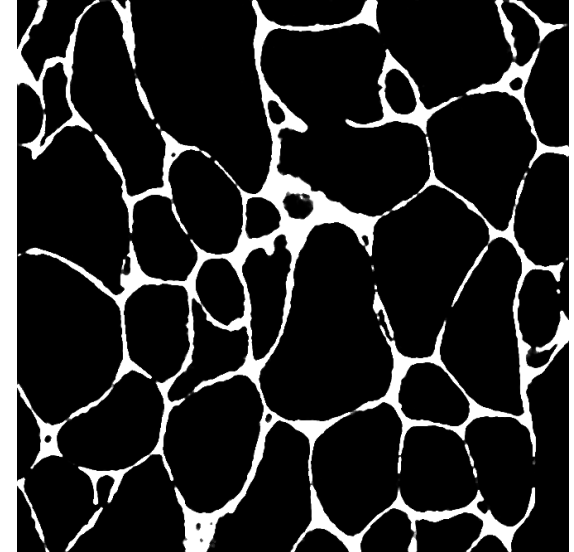
Processing of a Computer Tomography scan of a cellular metal



Gray-levels CT scan



Binary image



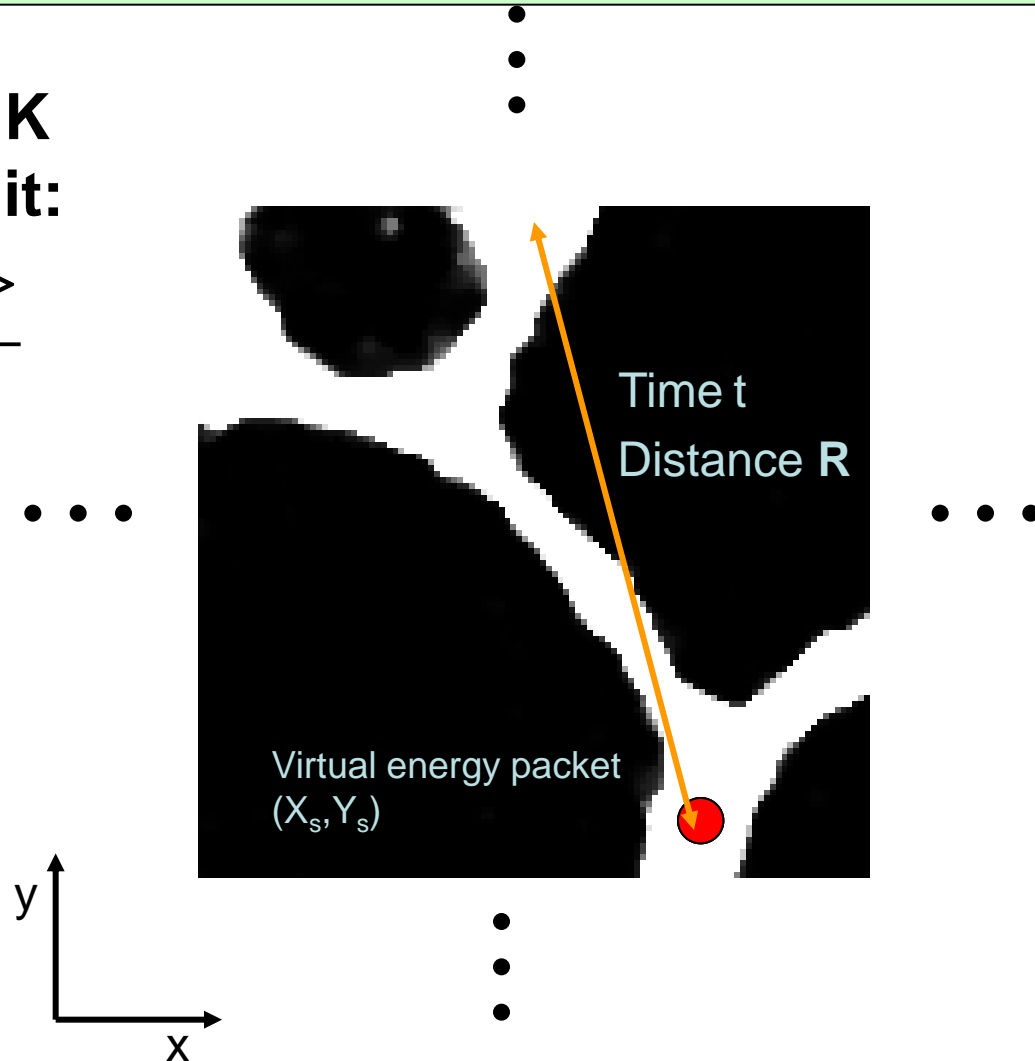
Filtered binary image

The filtered binary image is then mapped one-to-one onto the LMC lattice.

LMC determination of the effective thermal diffusivity / conductivity of a cellular metal.

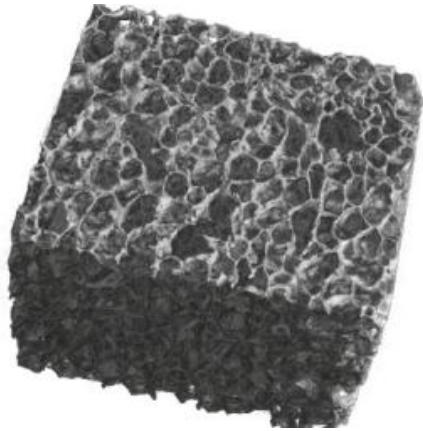
Thermal diffusivity K
in the long-time limit:

$$K = \frac{\langle R^2 \rangle}{6t}$$



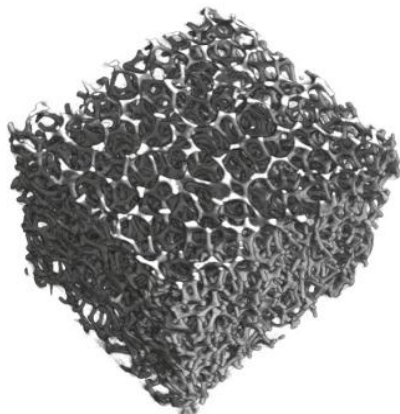
Determination of the thermal conductivity of two CT-scanned cellular metals compared with experimental measurements

on the same material, Fiedler, Belova, Murch, Oechsner, AEM, 2008.



M-pore

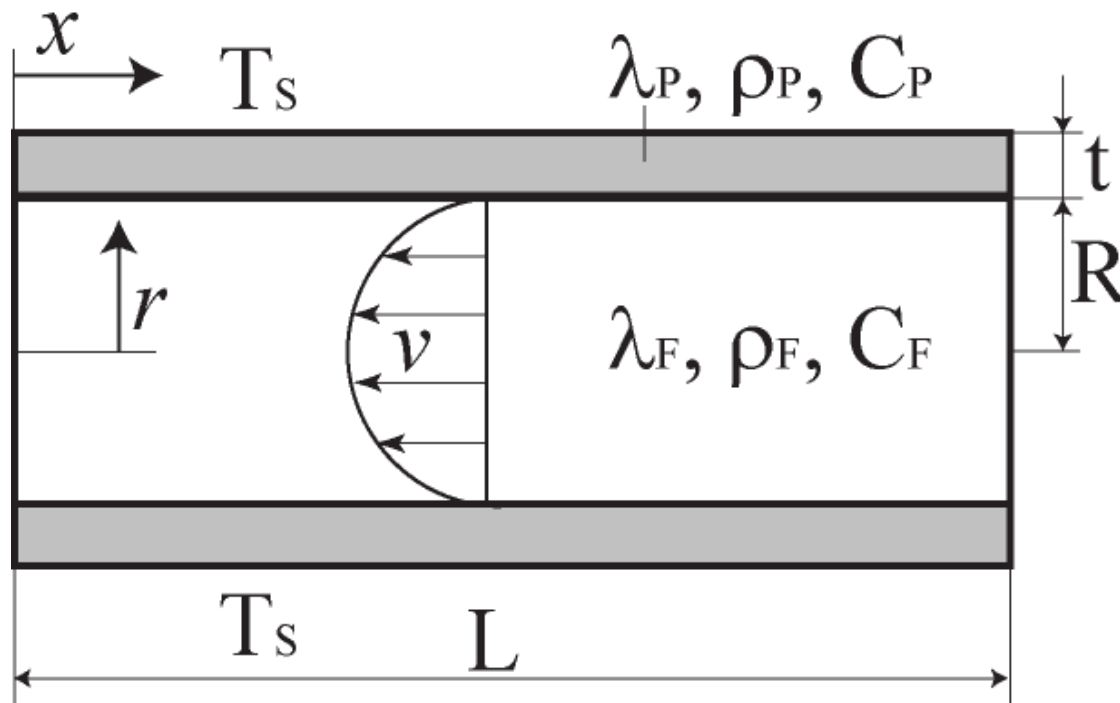
Expt.	CT scans and Lattice Monte Carlo
6.8 ± 0.5	6.5
W/(m.K)	W/(m.K)



Alporas

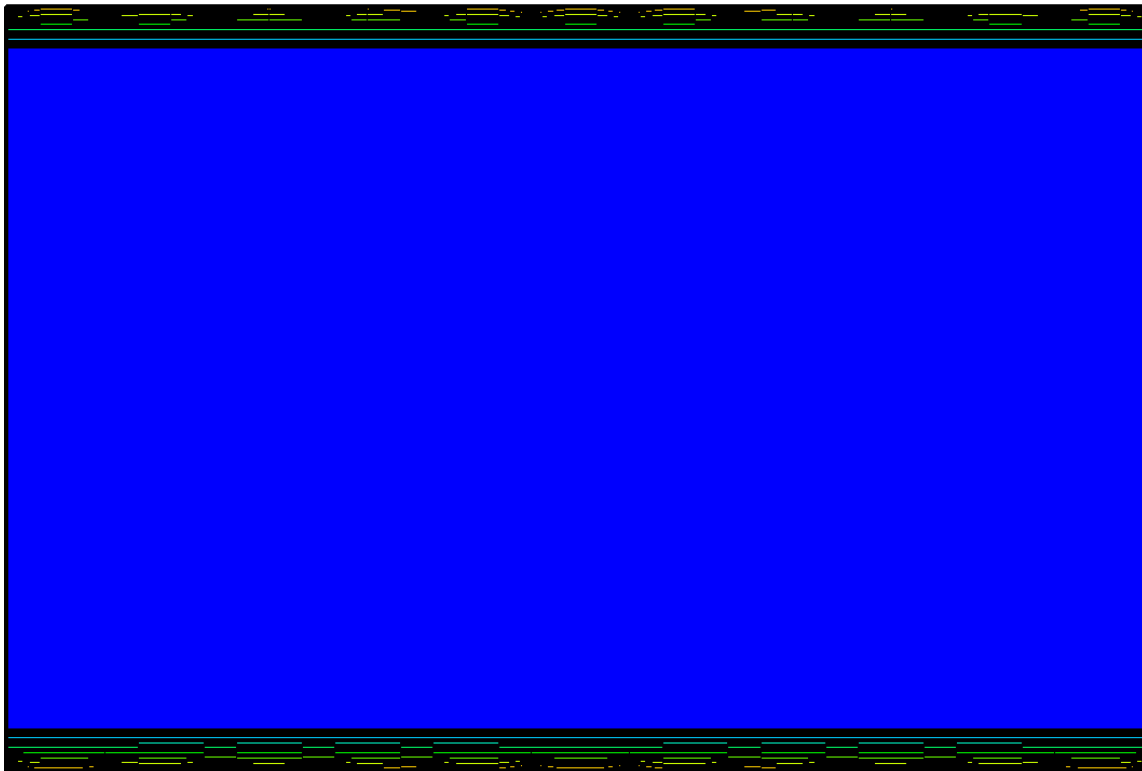
Expt.	CT scans and Lattice Monte Carlo
3.5 ± 0.3	3.2
W/(m.K)	W/(m.K)

Coupled heat conduction and laminar flow



Fluid velocity profile: Hagen-Poiseuille equation

LMC generated temperature field



Concluding remarks

Advantages:

- Very straightforward to program (codes are usually no more than 120 lines in C++ or FORTRAN).
- Extremely robust, can readily address non-linear diffusion problems.
- Because it is a quasi simulation, one quickly obtains a 'physical feel' for the problem.
- Very memory efficient.
- Avoids the meshing problems in FEA.

Disadvantages:

- Computationally quite intensive, several hours per run (e.g. to get a profile) are required on a high-end PC.
- No commercial LMC software available yet.
- MATLAB is unsuitable for LMC because of the very slow generation of random numbers.

Likely extensions and new applications of the LMC method

- Address moving boundary problems in mass diffusion by way of a moving reference frame. **Work in progress: (uses a combination of 'lattice' volume elements and continuous random walks of mass packets.**
- Address mathematically related phenomena such as the effective magnetic permeability, dielectric and elastic properties etc of composites etc.
- Using 3D X-ray Diffraction (3DXRD), it will soon be possible to routinely get 3D grain boundary maps of some metals. Assuming the same grain boundary diffusivity for all grain boundaries the application of the same LMC procedures for describing thermal transport in cellular metals would give a prediction of effective diffusivities and grain boundary diffusion penetration into real polycrystalline metals .

Thank you for your attention!